DOI:10.1130/GES01102.S2

Supplementary material for: Long, S.P., 2015, An upper-crustal fold province in the hinterland of the Sevier orogenic belt, eastern Nevada, U.S.A.: a Cordilleran Valley and Ridge in the Basin and Range: Geosphere, v. 11, doi:10.1130/GES01102.1.

Section SM1: Stereoplots supporting dip magnitude maps.

Figure SM1: Equal-area, lower-hemisphere projections, generated using Stereonet 8 (Allmendinger et al., 2011), showing poles-to-planes of bedding for Paleozoic-Mesozoic rocks (red dots) and bedding, compaction foliation, and flow foliation for Tertiary rocks (black triangles), which were used to calculate the mean attitudes that support the dip magnitude maps shown on Figures 3A-C and Figure SM2. Attitudes were measured directly off of source maps, which are listed in the name of the stereoplot. The number of analyses and the age range of rocks that attitudes were measured on are shown at the bottom of each stereoplot. Average attitudes were calculated using the mean vector (m.v.) function, which are shown as strike and dip symbols on Figure 3A for Tertiary rocks, and on Figure SM2 for Paleozoic-Mesozoic rocks. Red boxes represent the mean vector for Paleozoic-Mesozoic rocks, and black boxes represent the mean vector for Tertiary rocks. Ellipses represent the 95% confidence interval corresponding to each mean vector. For stereoplots that have both Paleozoic-Mesozoic and Tertiary attitudes plotted, Paleozoic-Mesozoic attitudes were rotated to their Paleogene attitude by using the 'rotate data' function to rotate the mean attitude of Tertiary rocks to horizontal, and rotate Paleozoic-Mesozoic rocks by the same amount. The un-rotated data are shown on their own stereoplots (marked with '_rotated' at the end of their name). The resulting Paleogene mean attitudes for Paleozoic-Mesozoic rocks are shown as strike and dip symbols on Plate 1 and Figure 3C.

Figure SM2: Dip magnitude map, covering the same area as Plate 1, showing present day attitudes of Paleozoic-Mesozoic rocks (see Plate 1 for structure abbreviations). Colored polygons represent areas on source mapping where multiple measurements demonstrate that rocks consistently have a similar attitude. Areas with variable attitude or insufficient attitude data are not shown. Strike and dip symbols represent the mean attitude of multiple measurements, which are plotted on Figure SM1; brown numbers next to strike and dip symbols correspond to individual stereoplots in Figure SM1. Figure 3B in the text shows a similar dip magnitude map for Paleozoic-Mesozoic rocks, with strike and dip symbols omitted for simplicity.

Section SM2: Zipped ArcGIS files accompanying Plate 1; includes mxd document and shapefiles.

Figure SM3: This version of Plate 1 is designed as an interactive PDF that allows examination of layers of specific spatial data sets individually. To see the list of available layers, click on the 'layers' tab in the left-hand table of contents in the PDF viewer. Layers of interest can be turned on and off by clicking on the eye symbol to the left of the name of the appropriate layer.

Section SM3: Detailed descriptions of ENFB and CNTB structures.

1. FIRST-ORDER FOLDS OF THE EASTERN NEVADA FOLD BELT

1.1. Pinto Creek syncline

The axis of a north-trending syncline, which preserves rocks as young as Permian and Cretaceous in its hinge zone, can be traced for ~95 km from the northern Pancake Range through the full length of the Diamond Mountains (Plate 1). Nolan et al. (1974) referred to the portion of this fold in the southern Diamond Mountains as the Pinto Creek syncline, and this name is applied here to its full length. In the northern Diamond Mountains, the Pinto Creek syncline has an eastern limb that dips 25–40° west and a western limb that steepens progressively toward the south, from 25° east to 80° east. At the northern end of the range, retro-deformation of tilts of Tertiary rocks indicates original western and eastern limb dips of ~25° southeast and ~50° southwest, respectively. In addition to the Pinto Creek syncline, the axes of several 2nd-order folds can be traced for distances up to 10–15 km in the northern half of the range.

In the southern Diamond Mountains, the western limb of the Pinto Creek syncline dips between 60° east and 80° west (overturned), and the eastern limb dips ~20° northwest. The axis is jogged to the north by offset and differential erosion across a west-dipping normal fault (Nolan et al., 1971), and reappears within the Newark Canyon Formation on the western flank of the range. From here, the axis can be traced to the southeast corner of the range, where the western limb dips 30–50° northeast and the eastern limb dips 20° northwest. Because the Paleogene unconformity is untilted in the southern Diamond Mountains (Long et al., 2014), these limb orientations approximate the pre-Paleogene fold geometry. In the northern Pancake Range, the western limb dips ~15° east and the eastern limb dips ~20° west. At the southern end of its axial trace, retro-deformation of Tertiary tilts indicates Paleogene western and eastern limb dips of ~10° east and ~40° west, respectively.

The amplitude of the Pinto Creek syncline, as estimated from cross-sections on source maps, ranges between 1400 and 3000 m, and the amplitudes of 2nd-order folds in the northern Diamond Mountains range between 500 and 1500 m. The pre-extensional wavelength of the Pinto Creek syncline, as estimated from the restored map distance between the axes of the adjacent Eureka culmination to the west and Illipah anticline to the east (Fig. 6), is 25–35 km. The syncline folds the Aptian (~122–116 Ma) Newark Canyon Formation in the southern Diamond Mountains (Long et al., 2014), and folds undated rocks mapped as Newark Canyon Formation in the northern Diamond Range (Stewart and Carlson, 1978). Long et al. (2014) interpreted the portion of the Pinto Creek syncline in the southern Diamond Mountains as the frontal axis of a hanging wall ramp above the Ratto Canyon thrust, and therefore as an Aptian fold that grew synchronous with Newark Canyon Formation deposition. However, the construction mechanism for this fold further north in the Diamond Mountains is unclear, as no thrust faults are exposed through a complete section of Silurian through Permian rocks in its western limb (Nolan et al., 1971), and the geometry changes to a much tighter fold with steeper limbs and multiple subsidiary folds.

1.2. Illipah anticline

In the White Pine Range, Humphrey (1960) mapped the north-trending Illipah anticline. Compilation of mapping along-trend in the White Pine Range (Moores et al., 1968; Tracy, 1969; Hose and Blake, 1976; Guerrero, 1983) and to the north along Alligator Ridge and Bald Mountain (Nutt, 2000; Nutt and Hart, 2004) shows that this fold can be traced for ~105 km, and the name Illipah anticline is here applied along its full length. Along Bald Mountain and Alligator Ridge, the axis can be traced discontinuously, with modern western and eastern limb dips of ~20°west and ~15–40° east, respectively. In the White Pine Range, the western limb dips ~20–35° west and the eastern limb dips ~40–45° east. At Paleogene erosion levels, Devonian to

Mississippian rocks were exposed in the hinge zone, and rocks ranging from Pennsylvanian to Triassic were preserved in the limbs.

Retro-deformation of tilts of Tertiary rocks indicates original limb dips between ~15–35° west for the western limb, and ~15–30° east for the eastern limb. The amplitude, as estimated from Paleogene structural relief, was between 1200 and 2050 m in the western limb, and between 2300 and 3800 m in the eastern limb. The pre-extensional wavelength, estimated between the axes of the adjacent Pinto Creek syncline and Butte synclinorium, is 35–50 km. Rocks as young as Lower Triassic are folded in the eastern limb of the Illipah anticline, providing a maximum age bound.

West of the Illipah anticline axis in the White Pine Range, several 2nd-order folds are present. The largest of these is the Little Antelope syncline (Humphrey, 1960), which can be traced for 50 km, preserves rocks as young as Permian in its hinge zone, and has modern western and eastern limb dips between 20 and 65° east and 20–35° west, respectively. Its Paleogene amplitude varies between 620 and 1050 m, and its minimum wavelength is 4–7 km. In addition, several other 2nd-order folds in the White Pine Range can be traced for map distances of 8–10 km, with modern wavelengths between 2 and 9 km (Humphrey, 1960; Guerrero, 1983; Tracy, 1969; Moores et al., 1968), and maximum Paleogene amplitudes between 300 and 600 m.

1.3. Butte synclinorium

Hose (1977) documented that rocks as young as Permian and Triassic are preserved in a 200 km long, north to north-northwest trending map pattern that trends through the Butte Mountains, central Egan Range, and southern Schell Creek Range, and designated this the ‘Butte structural trough’. Gans and Miller (1983) later referred to this structure as the ‘Butte synclinorium’, and show it as a regional syncline. Long (2012) extended the map pattern of the Butte synclinorium, and showed that it can be traced for ~250 km on the basis of Paleogene subcrop patterns.

Formation-scale subcrop patterns of an 80 km length of the Butte synclinorium are shown on Plate 1. At Paleogene erosion levels, up to 900 m of Triassic rocks are preserved in its hinge zone in the Maverick Springs Range and the Butte Mountains, as well as a complete section of Permian rocks that is up to 2750 m-thick (Stewart, 1980). In the Butte Mountains, modern western and eastern limb dips are 20–30° east and 25–30° west, respectively. In addition, Douglass (1960) mapped a series of 2nd-order folds in the southern Butte Mountains, which can be traced for map distances of 5–10 km, have limbs with a total dip range between 15 and 30°, modern wavelengths between 1 and 4 km, and Paleogene amplitudes between 250 and 700 m. To the south, along Radar Ridge, the master structure of the Butte synclinorium is referred to as the Radar Ridge syncline (Brokaw and Barosh, 1968), and has a modern western limb dip between 35 and 50° east, and a modern eastern limb dip that varies between 30° west and overturned.

The Paleogene amplitude of the Butte synclinorium was between 2300 and 3800 m, and its Paleogene wavelength is 25–45 km. The Butte synclinorium folds rocks as young as Lower Triassic, providing a maximum age bound.

1.4. Cherry Creek anticline

The subcrop pattern of a north-trending anticline is defined east of the axis of the Butte synclinorium on the subcrop map of Long (2012), although it was not formally named or described. It is defined by Devonian, Mississippian, and Pennsylvanian erosion levels juxtaposed between the Permian to Triassic erosion levels of the adjacent Butte and Pequop synclinoria, which can be traced for 110 km on the map of Long (2012), from southern Butte Valley, and

through the Cherry Creek and northern Egan ranges. This fold is here named the Cherry Creek anticline.

The southern 30 km of the Cherry Creek anticline axis is present on the northeast edge of Plate 1, where the western limb has a modern limb dip of 25–30° west. Retro-deformation of Tertiary tilts defines a Paleogene western limb dip of 15–20° west, and data from the subcrop map of Gans and Miller (1983) define a Paleogene eastern limb dip of 10–35° east. The amplitude of the western limb is 2300–3800 m at its southern extent on Plate 1. To the northeast of Plate 1, the total amplitude of the Cherry Creek anticline is between 3100 and 4000 m, and decreases to 2700 m at its northern extent. The Paleogene amplitude, estimated between the axes of adjacent 1st-order folds, is 15–40 km. Rocks folded in the hinge zone that are mapped as the Lower Jurassic Aztec sandstone (Coats, 1987) provide a maximum age bound.

1.5. Pequop synclinorium

The Pequop synclinorium was defined on the subcrop map of Long (2012), based on a north-trending subcrop pattern of Permian, Triassic, and Jurassic rocks preserved for a distance of 115 km, from the northern Schell Creek Range to the southern Pequop Mountains. Paleogene limb dips are estimated from retro-deformed attitudes presented in Gans and Miller (1983) for the southern ~30 km of the fold in the Schell Creek Range, and vary between 10 and 35° east in the western limb, and 25–30° west in the eastern limb. The Paleogene amplitude is 2500–3000 m at its southern end, and as high as 3400–4000 m at its northern end. The Paleogene wavelength, estimated between the axes of the Cherry Creek anticline and Confusion synclinorium, has to be less than 25 km. Rocks as young as Lower Jurassic (Coats, 1987) are folded in the shared limb of the Pequop synclinorium and Cherry Creek anticline, which provides a maximum age bound.

2. THRUST FAULTS AND FOLDS OF THE NORTHERN CENTRAL NEVADA THRUST BELT

2.1. Eureka culmination and associated structures

In the northern Fish Creek Range and southern Diamond Mountains, Paleogene erosion levels vary between Cambrian and Permian, indicating a total structural relief of ~6 km. Using retro-deformed cross-sections, Long et al. (2014) showed that the pre-extensional deformation geometry across the two ranges defines the Eureka culmination, an anticline with a ~20 km wavelength, a ~4.5 km amplitude, and limb dips of ~25–35°. A Cambrian over Silurian relationship defined in drill holes under the anticline crest (same location as stereoplots 24 and 25) is interpreted as the east-vergent, blind Ratto Canyon thrust, and the Eureka culmination is interpreted as a fault-bend fold constructed by ~9 km of eastward motion of the Ratto Canyon thrust sheet over a footwall ramp that cuts upsection toward the east from Cambrian to Silurian rocks (Long et al., 2014). Stratigraphic throw on the Ratto Canyon thrust is estimated at 2000–2500 m where it is drilled, where Middle Cambrian rocks are in its hanging wall, but may be as high as 3500 m ~5 km to the north, where rocks as deep as Lower Cambrian are exposed. Long et al. (2014) proposed that the type-section of the Early Cretaceous (Aptian, ca. 116–122 Ma; Druschke et al., 2010) Newark Canyon Formation was deposited in a piggyback basin that developed on the eastern limb of the Eureka culmination as it grew.

After its construction, the Eureka culmination underwent 7–8 km (40%–45%) of extension, accommodated by two sets of normal faults that pre-date late Eocene (~37 Ma) volcanism (Long et al., 2014). Therefore, the complex subcrop pattern illustrated on Plate 1 is the cumulative result of erosional exhumation of the culmination during and after its construction, and tectonic exhumation by pre-volcanic normal faults. The earliest extension,

which is bracketed as post-Aptian (<116 Ma) and pre-late Eocene (>37 Ma) was accommodated by low cutoff-angle normal fault systems, including the down-to-the-east Hoosac fault system in the eastern limb (Plate 1). The second episode of extension is bracketed between Late Cretaceous (<84–72 Ma) and late Eocene (>37 Ma), and was accommodated by down-to-the-west normal faults, including the Pinto Summit and Dugout Tunnel faults (Plate 1). The second episode of extension was accompanied by 20–30° of eastward tilting, which steepened the eastern limb from an original dip of ~20–40° east to as high as 60–70° east (stereoplots 24, 26–28), and shallowed the western limb from an original dip of ~30–40° west to 15–20° west (stereoplots 16, 18, 20) (Long et al., 2014).

The Eureka culmination can be traced for a minimum north-south distance of 80 km, from Devonian subcrop levels in drill holes in Diamond Valley (Hess et al., 2004) to subcrop levels as deep as Ordovician in the northern Pancake Range (Kleinhampl and Ziony, 1985). The deep erosion levels in the Pancake Range are spatially associated with the trace of the Moody Peak thrust, discussed in section 5.3.3 below.

Within the eastern limb of the Eureka culmination, the steeply west-dipping Moritz-Nager thrust (French, 1993) places Devonian rocks over Mississippian rocks (Plate 1) (Long et al., 2014). The Moritz-Nager thrust exhibits 1000–1300 m of stratigraphic throw, has an estimated 1–2 km of top-to-the-east displacement, and is interpreted as a subsidiary structure that post-dates the majority of motion on the Ratto Canyon thrust (Long et al., 2014).

2.2. Antelope thrust

In the northern Antelope Range, Hose (1983) mapped a thrust fault that places Cambrian rocks over Mississippian rocks, and Carpenter et al. (1993) named this structure the Antelope thrust (Plate 1). This thrust ramps upsection toward the east through Mississippian rocks in its footwall (Hose, 1983), and is interpreted here as east-vergent. At Paleogene erosion levels, Ordovician rocks were exposed at the surface in its hanging wall (Plate 1). Based on differences in the stratigraphic section between the Antelope Range and Fish Creek Range, Hose (1983) suggested that a thrust fault may be concealed between the two ranges. After this suggestion, the trace of the Antelope thrust is approximated between the two ranges (Plate 1), and is shown connecting to the south with a Devonian over Pennsylvanian-Permian thrust fault mapped in the Park Range by Dixon et al. (1972). Throw on the Antelope thrust is ~2600 m in the northern Antelope Range, and decreases to ~900–1400 m in the Park Range.

2.3. Northern Pancake Range

The northern Pancake Range suffers from a dearth of detailed bedrock mapping, and different naming schemes for folds and thrust faults have been previously proposed (Nolan et al., 1974; Carpenter et al., 1993; Ransom and Hansen, 1993; Long, 2012). Here, a new naming and correlation scheme is proposed, based on primary map sources (Nolan et al., 1974; McDonald, 1989), with additions from Carpenter et al. (1993).

1. Moody Peak thrust. In the northwest corner of the range, Kleinhampl and Ziony (1985) mapped Cambrian and Ordovician rocks in thrust contact over Devonian rocks, and Carpenter et al. (1993) described this structure as the east-vergent Moody Peak thrust. Based on interpolation of subcrop data (Plate 1), the Moody Peak thrust is shown with a footwall flat in the Devonian Nevada Formation, and ramping upsection toward the east in its hanging wall from Silurian to Ordovician rocks. Stratigraphic throw across the Moody Peak thrust is estimated between 700 and 1750 m. Carpenter et al. (1993) stated that the Moody Peak thrust cuts undated rocks mapped as the Newark Canyon Formation. However, given the difficulties in correlating rocks without precise age control that are mapped as Newark Canyon Formation (e.g., see discussion

in the main body of this manuscript and in Long et al. [2014]), the Early Cretaceous maximum motion age constraint that this field relationship implies is considered tentative.

Based on their spatial relationships to deep erosion levels associated with the Eureka culmination, and the relative stratigraphic levels that they deform, the Moody Peak and Ratto Canyon thrust faults are correlated here. The southward decrease in throw between these two structures is consistent with their relative hanging wall and footwall stratigraphic levels. Under this correlation, the combined Ratto Canyon-Moody Peak thrust can be traced for a minimum north-south distance of 40 km.

2. Pancake thrust system. In the northwest Pancake Range, Nolan et al. (1974) mapped two thrust faults, one west-dipping and one east-dipping, that place Devonian rocks over Mississippian rocks. Carpenter et al. (1993) interpreted both of these structures as a single, folded, east-vergent thrust fault named the Pancake thrust. These two thrust traces connect to the south with the east-vergent Red Ridge-Lost Hills thrust system described by McDonald (1989). In this study, the Pancake thrust and Red Ridge-Lost Hills thrust system are correlated, and referred to as the Pancake thrust system. The Pancake thrust system can be traced for a north-south distance of ~35 km, and stratigraphic throw on individual structures varies between 300 and 1300 m. Structures of the Pancake thrust system cut rocks as young as Mississippian, and are truncated by an Aptian (108 ± 3 Ma; K-Ar biotite; Nolan et al., 1974) dacite stock (McDonald, 1989).

3. Green Springs thrust. McDonald (1989) mapped the northeast-striking, east-vergent Green Springs thrust, which is interpreted to be structurally higher than the Pancake thrust system. At Paleogene erosion levels, the thrust places Devonian and Lower Mississippian rocks over Upper Mississippian rocks, corresponding to a range in stratigraphic throw between 600 and 1500 m. Undated conglomerate mapped as the Newark Canyon Formation overlaps the Green Springs thrust (McDonald, 1989); however, similar to the discussion above for the Moody Peak thrust, without precise age control on these rocks, this age constraint should be considered tentative.

4. Duckwater thrust. The east-vergent Duckwater thrust was first described by Carpenter et al. (1993), and places Devonian and Lower Mississippian rocks over Upper Mississippian, Pennsylvanian, and Permian rocks (Plate 1), corresponding to a range in throw between ~1500–2100 m. The Duckwater thrust can be traced for a minimum of ~30 km north to south, and is speculatively traced an additional 10 km to the north into Newark Valley on basis of subcrop patterns (Plate 1). The Duckwater thrust cuts rocks as young as Lower Permian.

2.4. Central Pancake Range and Railroad Valley

Extensive cover under Tertiary volcanic rocks makes construction of an accurate subcrop map for much of the central Pancake Range difficult. However, Paleogene subcrop patterns in Railroad Valley are aided by extensive drill hole data from petroleum exploration (French, 1998; Hess et al., 2004). In most areas, subcrop patterns were interpreted as representing erosionally beveled folds, because of a lack of evidence for older over younger structural relationships in drill hole data in Railroad Valley (e.g., French, 1998).

1. Portuguese Mountain thrust. A northeast-striking, east-vergent thrust fault was mapped by Quinlivan et al. (1974), and is here named the Portuguese Mountain thrust. At Paleogene erosion levels, it places Devonian and Lower Mississippian rocks over Upper Mississippian rocks, corresponding to a range in throw between 250 and 1350 m.

2. McClure Spring syncline. The north-northwest trending McClure Spring syncline was described west of the town of Duckwater by Perry and Dixon (1993), where it contains

Pennsylvanian, Permian, and Cretaceous rocks in its hinge zone. Here, the fold has a vertical to overturned western limb, an eastern limb that dips up to 50°W, and is interpreted as east-vergent (Perry and Dixon, 1993). Kleinhampl and Ziony (1985) mapped the Cretaceous Newark Canyon Formation in its hinge zone; these rocks are mapped as Cretaceous because they have yielded dinosaur bones, but they cannot be more precisely dated. Perry and Dixon (1993) argued that Permian rocks are the youngest involved in folding, and while Cretaceous rocks are present, they are not involved in folding, and overlap folded Pennsylvanian rocks across a ~90° angular unconformity. The syncline can be traced ~30 km to the south through Railroad Valley, where Mississippian rocks occupy the hinge zone, and the eastern and western limbs are defined by erosion levels that descend downsection to Devonian rocks. Rocks in the western limb presently dip ~25–40° east, and restore to Paleogene dips of ~10–15° northeast. The amplitude of the fold varies from 1100 to 1400 m at its northern and southern ends, to a maximum of 2100–2600 m where Permian rocks are preserved in its hinge zone.

3. Trap Spring anticline. A north-trending anticline can be traced for ~70 km on the basis of an elongate subcrop pattern of Devonian rocks in Railroad Valley and the central Pancake Range, which climbs upsection to the west and east to units as young as Mississippian, Pennsylvanian, and Permian. This fold was originally defined on a subcrop map of Railroad Valley by French (1998), and is here named the Trap Spring anticline because of its proximity to the Trap Spring oil field. The amplitude ranges between 600 and 1300 m in Railroad Valley, to a maximum of 2600 m where Permian rocks are preserved in its western limb.

4. Bacon Flat syncline. A north to north-northwest trending syncline can be traced for ~70 km along the eastern side of Railroad Valley and through the Duckwater Hills, on the basis of an elongate subcrop pattern preserving rocks as young as Pennsylvanian, which descends to Devonian levels in the western limb and Devonian to Mississippian levels in the eastern limb. This syncline was originally defined on a subcrop map of Railroad Valley by French (1998), and is referred to here as the Bacon Flat syncline, after its proximity to the Bacon Flat oil field. The amplitude varies between 600 and 1500 m.

2.5. Quinn Canyon Range and southern Grant Range

Three east-vergent CNTB thrust faults are mapped in the Quinn Canyon Range and southern Grant Range (listed here from structurally-highest to lowest):

1. Sawmill thrust: The north-northeast striking Sawmill thrust places Ordovician rocks over Devonian rocks at Paleogene erosion levels (Bartley and Gleason, 1990), corresponding to a range in throw between 1250 and 3050 m. The Sawmill thrust can be traced for ~20 km, and cuts rocks as young as upper Devonian.

2. Rimrock thrust: The Rimrock thrust (Bartley and Gleason, 1990) is the northernmost segment of the Rimrock-Lincoln-Freiberg thrust system (Fig. 5), which is one of two through-going CNTB thrust systems that connect southward with structures of the Sevier thrust belt (Taylor et al., 2000; Long, 2012); the other is the Golden Gate-Mount Irish-Pahranagat thrust system (Fig. 5), which tips out 10 km south of Plate 1 (Armstrong and Bartley, 1993). At Paleogene erosion levels, the Rimrock thrust places Lower Devonian rocks over Upper Devonian rocks (Ekren et al., 2012), corresponding to a throw between 650 and 1200 m (Bartley and Gleason, 1990). 30–40 km south of Plate 1, structures associated with the correlative Lincoln thrust cut rocks as young as Pennsylvanian, and are cross-cut by a Late Cretaceous (ca. 90–98 Ma; K-Ar biotite) granite pluton (Taylor et al., 2000).

3. Schofield Canyon thrust and Timber Mountain anticline: In the southern Grant Range, the Schofield Canyon thrust places Cambrian rocks over Ordovician rocks, with an estimated

stratigraphic throw of 2700 m (Fryxell, 1988; 1991). Based on available subcrop data, the Schofield Canyon thrust was not erosionally-breached by the Paleogene (Plate 1). The Timber Mountain anticline, a recumbent hanging wall fold, is interpreted to be genetically related to motion on the Schofield Canyon thrust (Fryxell, 1988). The axis of the anticline is cross-cut by the Late Cretaceous (86.4 ± 4.6 Ma; U-Pb zircon) Troy granite stock (Taylor et al., 2000).

REFERENCES CITED

Allmendinger, R.W., Cardozo, N., and Fisher, D., 2011, Structural geology algorithms: Vectors and tensors in structural geology: New York, Cambridge University Press, 304 p.

Armstrong, P.A., and Bartley, J.M., 1993, Displacement and deformation associated with a lateral thrust termination, southern Golden Gate Range, southern Nevada, U.S.A: Journal of Structural Geology, v. 15, p. 721–735, doi:10.1016/0191-8141(93)90058-I.

Bartley, J.M., and Gleason, G.C., 1990, Tertiary normal faults superimposed on Mesozoic thrusts, Quinn Canyon and Grant Ranges, Nye County, Nevada: in Wernicke, B.P., ed., Basin and Range Extensional Tectonics Near the Latitude of Las Vegas Nevada: Geological Society of America Memoir 176, 195–212.

Brokaw, A.L., and Barosh, P.J., 1968, Geologic map of the Riepetown quadrangle, White Pine County, Nevada: USGS Geologic Quadrangle Map GQ-758, 1:24,000-scale, 1 plate.

Carpenter, D.G., Carpenter, J.A., Dobbs, S.W., and Stuart, C.K., 1993, Regional structural synthesis of Eureka fold-and-thrust belt, east-central Nevada: in Gillespie, C. W., ed., Structural and stratigraphic relationships of Devonian reservoir rocks, east-central Nevada: Nevada Petroleum Society 1993 Field Conference Guidebook, p. 59–72.

Coats, R.R., 1987, Geology of Elko County, Nevada: Nevada Bureau of Mines and Geology Bulletin 101, 112 p.

Dixon, G.L., Hedlund, D.C., and Ekren, E.B., 1972, Geologic map of the Pritchards Station quadrangle, Nye County, Nevada: USGS Miscellaneous Geologic Investigations Map I-728, 1:48,000-scale, 1 plate.

Douglass, W.B., Jr., 1960, Geology of the southern Butte Mountains, White Pine County, Nevada: in Boettcher, J.W., and Sloan, W.W., Jr., eds., Guidebook to the Geology of East-Central Nevada: Intermountain Association of Petroleum Geologists, 11th Annual Field Conference, p. 181–185.

Druschke, P., Hanson, A.D., Wells, M.L., Gehrels, G.E., and Stockli, D., 2010, Paleogeographic isolation of the Cretaceous to Eocene Sevier hinterland, east-central Nevada: Insights from U-Pb and (U-Th)/He detrital zircon ages of hinterland strata: Geological Society of America Bulletin, v. 123, p. 1141–1160, doi:10.1130/B30029.1.

Ekren, E.B., Rowley, P.D., Dixon, G.L., Page, W.R., Kleinhampl, F.J., Ziony, J.I., Brandt, J.M.,, and Patrick, B.G., 2012, Geology of the Quinn Canyon Range and vininity, Nye and Lincoln Counties, Nevada: Southern Nevada Water Authority, Groundwater Resources Department, Water Resources Division, Document Number HAM-ED-0004, 60 p., 1 plate, 1:100,000-scale map.

French, D.E., 1993, Thrust faults in the southern Diamond Mountains, Eureka and White Pine counties, Nevada: in Gillespie, C. W., ed., Structural and stratigraphic relationships of Devonian reservoir rocks, east-central Nevada: Nevada Petroleum Society 1993 Field Conference Guidebook, p. 105–114.

French, D.E., 1998, Petroleum systems of the Great Basin: the Railroad Valley model, in French, D.E, and Schalla, R.A., eds., Hydrocarbon habitat and special geologic problems of the Great Basin: Nevada Petroleum Society 1998 Field Trip Guidebook, p. 38–56.

Fryxell, J .E, 1988, Geologic map and description of stratigraphy and structure of the west-central Grant Range, Nye County, Nevada: Geological Society of America Map and Chart Series MCH064, 16 p., 2 sheets, 1:24,000-scale.

Fryxell, J.E., 1991, Tertiary tectonic denudation of an igneous and metamorphic complex, west-central Grant Range, Nye County, Nevada: *in* Raines, G.L., et al., eds., Geology and Ore Deposits of the Great Basin: Symposium and Proceedings, Geological Society of Nevada, Reno, p. 87–92.

Gans, P.B., and Miller, E.L., 1983, Style of mid-Tertiary extension in east-central Nevada: Utah Geological and Mineral Survey Special Studies, v. 59, p. 107–160.

Guerrero, J.A., 1983, Geology of the northern White Pine Range, east-central Nevada [M.S. thesis]: California State University, Long Beach, 105 p., 3 plates, 1:24,000-scale map.

Hess, R.H., Fitch, S.P., and Warren, S.N., 2004, Nevada oil and gas well database: Nevada Bureau of Mines and Geology Open-File Report 04–1.

Hose, R.K., 1977, Structural geology of the Confusion Range, west-central Utah: U.S. Geological Survey Professional Paper, v. 971, p. 97–131.

Hose, R.K., 1983, Geologic map of the Cockalorum Wash quadrange, Eureka and Nye counties, Nevada: U.S. Geological Survey Miscellaneous Investigations Series Map I-1410, 1:31,680-scale, 1 plate.

Hose, R.K., and Blake, M.C., Jr., 1976, Geologic map of White Pine County, Nevada, USGS Open-File Report OF-70–166.

Humphrey, F.L., 1960, Geology of the White Pine Mining District, White Pine County, Nevada: Nevada Bureau of Mines and Geology Bulletin 57, 1:48,000-scale, 1 plate, 67 p.

Kleinhampl, F.J., and Ziony, J.L., 1985, Geology of northern Nye County, Nevada: Nevada Bureau of Mines Bulletin 99A, 171 p.

Long, S.P., 2012, Magnitudes and spatial patterns of erosional exhumation in the Sevier hinterland, eastern Nevada and western Utah, USA: Insights from a Paleogene paleogeologic map: Geosphere, v. 8, p. 881–901, doi:10.1130/GES00783.1.

Long, S.P., Henry, C.D., Muntean, J.L., Edmondo, G.P., and Cassel, E.J., 2014, Early Cretaceous construction of a structural culmination, Eureka, Nevada, U.S.A.: implications for out-of-sequence deformation in the Sevier hinterland: Geosphere, v. 10, p. 564–584, doi:10.1130/GES00997.1.

McDonald, S.F., 1989, Geology, Pogues Station quadrangle, White Pine and Nye Counties, Nevada [M.S. thesis], San Diego State University, 107 p.

Moores, E.M., Scott, R.B., and Lumsden, W.W., 1968, Tertiary tectonics of the White Pine Range-Grant Range region, east-central Nevada, and some regional implications: Geological Society of America Bulletin, v. 79, p. 1703–1726, doi:10.1130/0016-7606(1968)79[1703:TTOTWP]2.0.CO;2.

Nolan, T.B., Merriam, C.W., and Brew, D.A., 1971, Geologic map of the Eureka quadrangle, Eureka and White Pine counties, Nevada: U.S. Geological Survey Miscellaneous Investigations Series, Map I-612: 1:31,680-scale, 8 p., 2 plates.

Nolan, T.B., Merriam, C.W., and Blake, M.C., Jr., 1974, Geologic map of the Pinto Summit quadrangle, Eureka and White Pine counties, Nevada: U.S. Geological Survey Miscellaneous Investigations Series, Map I-793: 1:31,680-scale, 14 p., 2 plates.

Nutt, C.J., 2000, Geologic Map of the Alligator Ridge Area, Including the Buck Mountain East and Mooney Basin Summit Quadrangles and Parts of the Sunshine Well NE and Long Valley Slough Quadrangles, White Pine County, Nevada: USGS Geologic Investigation Series I-2691, 1:24,000-scale, 1 plate.

Nutt, C.J., and Hart, K.S., 2004, Geologic map of the Big Bald Mountain quadrangle and part of the Tognini Spring quadrangle, White Pine County, Nevada: Nevada Bureau of Mines and Geology Map 145, 1:24,000-scale, 1 plate.

Perry, W.J., and Dixon, G.L., 1993, Structure and time of deformation in the central Pancake Range, a geologic reconnaissance: in Gillespie, C.W., ed., Structural and stratigraphic relationships of Devonian reservoir rocks, east-central Nevada: Nevada Petroleum Society 1993 Field Conference Guidebook, p. 123–132.

Quinlivan, W.D., Rogers, C.L., and Dodge, H.W., 1974, Geologic map of the Portuguese Mountain quadrangle, Nye County, Nevada: USGS Miscellaneous Investigations Series Map I-804, 1:48,000-scale, 1 plate.

Ransom, K.L., and Hansen, J.B., 1993, Cretaceous transpressional deformation, Eureka County, Nevada: in Gillespie, C. W., ed., Structural and stratigraphic relationships of Devonian reservoir rocks, east-central Nevada: Nevada Petroleum Society 1993 Field Conference Guidebook, p. 89–104.

Stewart, J.H., 1980, Geology of Nevada: a discussion to accompany the Geologic Map of Nevada: Nevada Bureau of Mines and Geology Special Publication 4, 136 p.

Stewart, J.H., and Carlson, J.E., 1978, Geologic map of Nevada: U.S. Geological Survey in collaboration with Nevada Bureau of Mines and Geology, scale 1:500,000, 1 sheet.

Taylor, W.J., Bartley, J.M., Martin, M.W., Geissman, J.W., Walker, J.D., Armstrong, P.A., and Fryxell, J.E., 2000, Relations between hinterland and foreland shortening: Sevier orogeny, central North American Cordillera: Tectonics, v. 19, no. 6, p. 1124–1143, doi:10.1029/1999TC001141.

Tracy, W.C., 1969, Structure and stratigraphy of the central White Pine Range, east-central Nevada [M.S. thesis]: California State University, Long Beach, 66 p., 8 plates, 1:24,000-scale map.

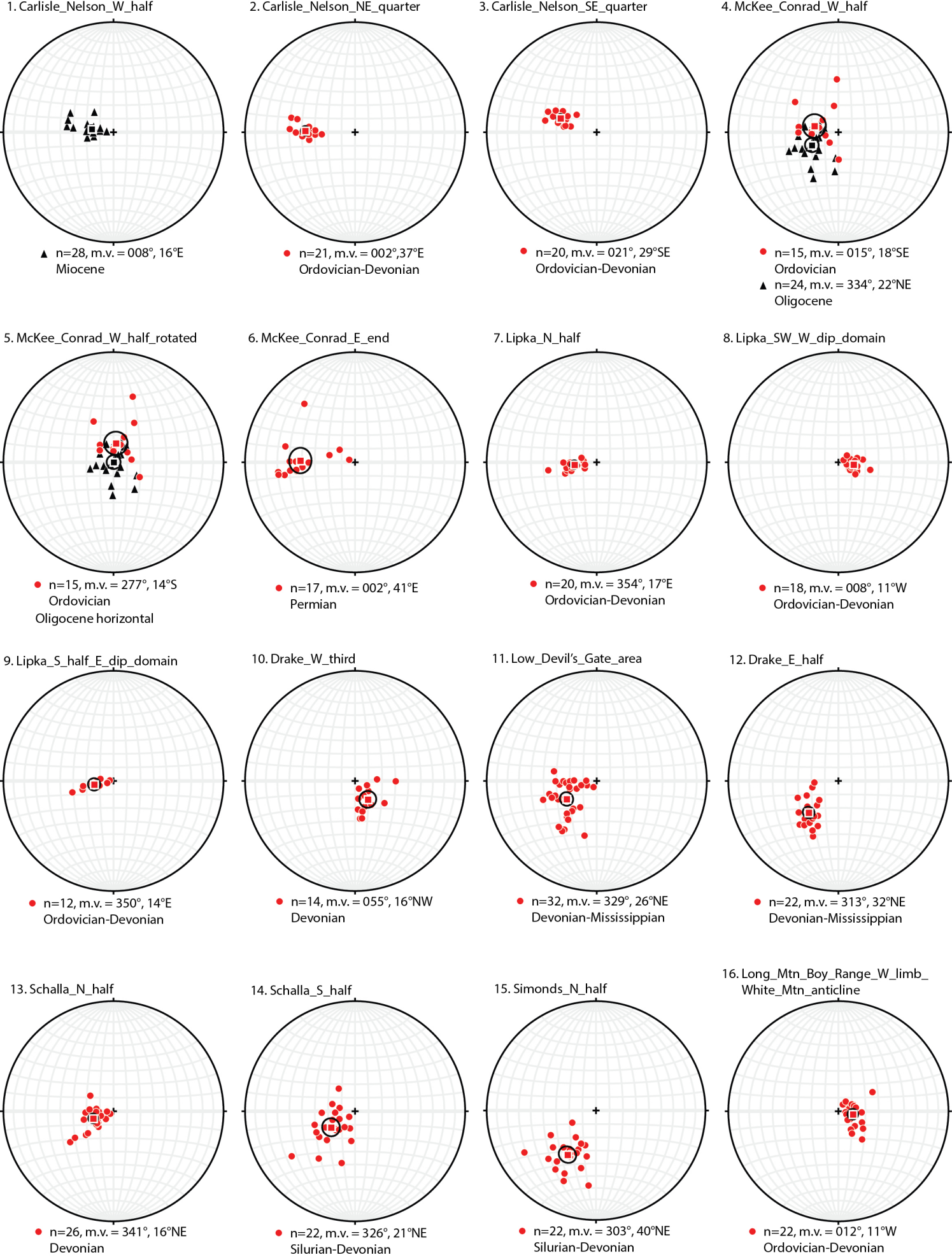
1. Carlisle_Nelson_W_half
n=28, m.v. = 008°, 16°E
Miocene
2. Carlisle_Nelson_NE_quarter
n=21, m.v. = 002°,37°E
Ordovician-Devonian
3. Carlisle_Nelson_SE_quarter
n=20, m.v. = 021°, 29°SE
Ordovician-Devonian
4. McKee_Conrad_W_half
n=15, m.v. = 015°, 18°SE
Ordovician
n=24, m.v. = 334°, 22°NE
Oligocene
5. McKee_Conrad_W_half_rotated
n=15, m.v. = 277°, 14°S
Ordovician
Oligocene horizontal
6. McKee_Conrad_E_end
n=17, m.v. = 002°, 41°E
Permian
7. Lipka_N_half
n=20, m.v. = 354°, 17°E
Ordovician-Devonian
8. Lipka_SW_W_dip_domain
n=18, m.v. = 008°, 11°W
Ordovician-Devonian
9. Lipka_S_half_E_dip_domain
n=12, m.v. = 350°, 14°E
Ordovician-Devonian
10. Drake_W_third
n=14, m.v. = 055°, 16°NW
Devonian
11. Low_Devil's_Gate_area
n=32, m.v. = 329°, 26°NE
Devonian-Mississippian
12. Drake_E_half
n=22, m.v. = 313°, 32°NE
Devonian-Mississippian
13. Schalla_N_half
n=26, m.v. = 341°, 16°NE
Devonian
14. Schalla_S_half
n=22, m.v. = 326°, 21°NE
Silurian-Devonian
15. Simonds_N_half
n=22, m.v. = 303°, 40°NE
Silurian-Devonian
16. Long_Mtn_Boy_Range_W_limb_
White_Mtn_anticline
n=22, m.v. = 012°, 11°W
Ordovician-Devonian

17. Long_Mtn_Boy_Range_E_limb_White_Mtn_anticline

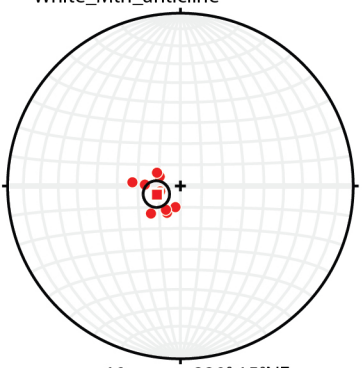

● n=10, m.v. = 330°,15°NE
Ordovician-Devonian

18. Long_Fish_Ck_Range_W_limb_White_Mtn_anticline

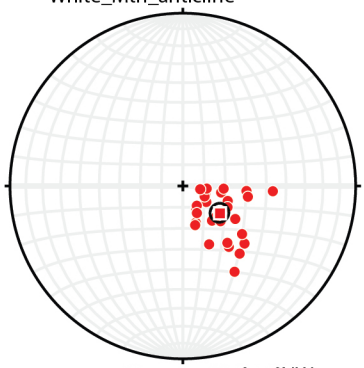

● n=32, m.v. = 036°,21°NW
Ordovician-Devonian

19. Long_Fish_Ck_Range_E_limb_White_Mtn_anticline

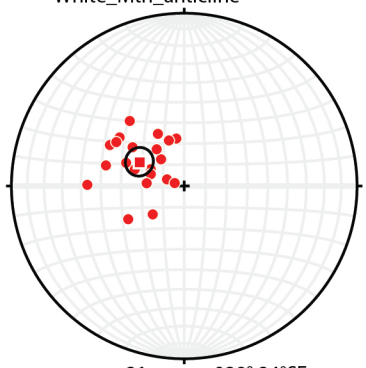

● n=21, m.v. = 028°,24°SE
Ordovician-Devonian

20. Cowell_W_limb_White_Mtn_anticline

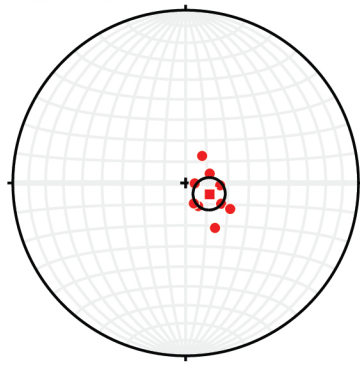

● n=9, m.v. = 025°,12°NW
Ordovician-Devonian

21. Cowell_E_limb_White_Mtn_anticline

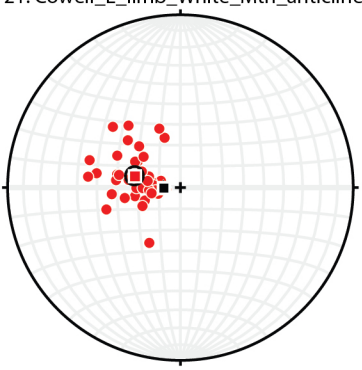

● n=39, m.v. = 014°, 22°SE
Ordovician-Devonian
▲ n=1, m.v. = 000°, 8°NE
Late Eocene

22. Cowell_E_limb_White_Mtn_anticline_rotated

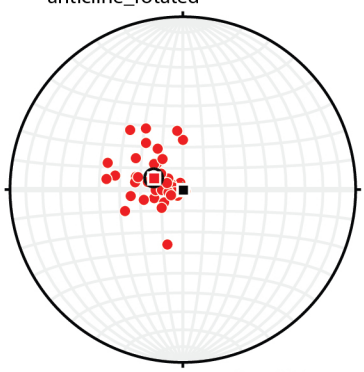

● n=39, m.v. = 022°, 15°SE
Ordovician-Devonian
Late Eocene horizontal

23. Nolan_1962_FW_Hoosac_fault

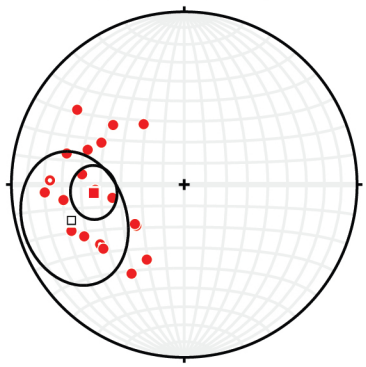

● n=21, m.v. = 353°, 53°E
Cambrian-Ordovician
Late Eocene volcanics approximately horizontal

24. Long_FW_Hoosac_flt_N_half

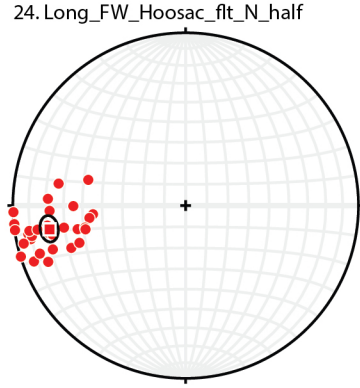

● n=32, m.v. = 350°, 69°E
Cambrian-Ordovician
Late Eocene volcanics approximately horizontal

25. Long_between_Dugout_Tunnel_and_Lookout_Mtn_faults

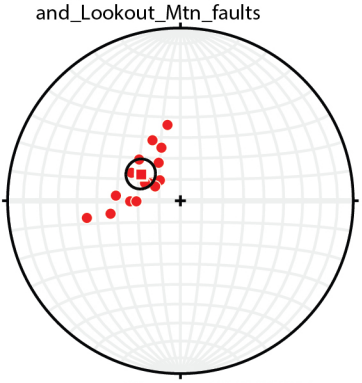

● n=18, m.v. = 034°, 23°SE
Cambrian-Ordovician
Late Eocene volcanics approximately horizontal

26. Long_FW_Hoosac_flt_S_half

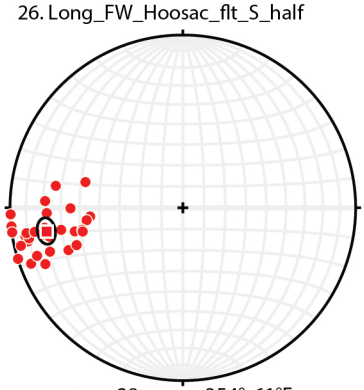

● n=28, m.v. = 354°, 61°E
Cambrian-Ordovician
Late Eocene volcanics approximately horizontal

27. Long_HW_Pinto_Summit_flt_middle

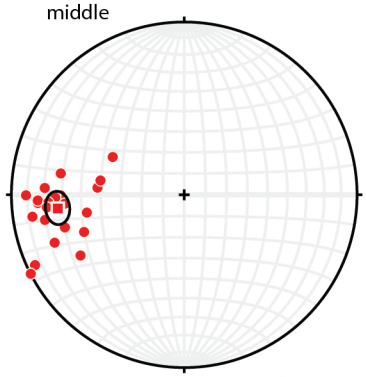

● n=24, m.v. = 354°, 63°E
Mississippian-Permian
Late Eocene volcanics approximately horizontal

28. Long_Nolan_1974_HW_Pinto_Summit_flt_S

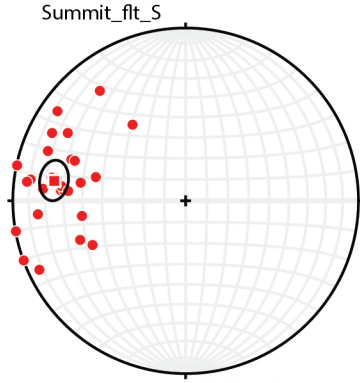

● n=27, m.v. = 008°, 66°E
Mississippian-Permian
Late Eocene volcanics approximately horizontal

29. Haworth_W_limb_Pinto_Ck_syncline_N_half

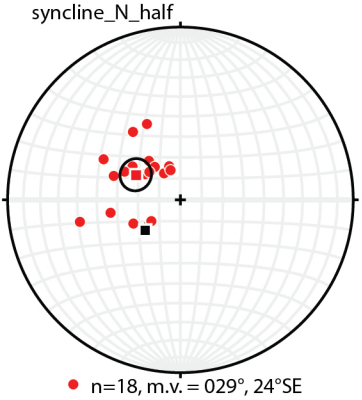

● n=18, m.v. = 029°, 24°SE
Mississippian-Pennsylvanian
▲ n=1, m.v. = 320°, 22°NE
Tertiary sediments

30. Haworth_W_limb_Pinto_Ck_syncline_N_half_rotated

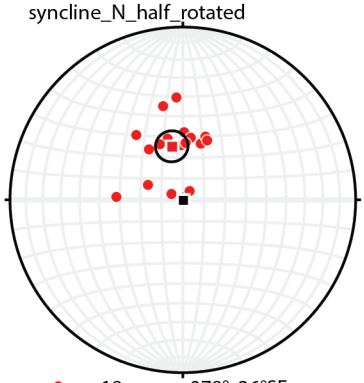

● n=18, m.v. = 078°, 26°SE
Mississippian-Pennsylvanian
Tertiary sediments horizontal

31. Haworth_E_limb_Pinto_Ck_syncline_N_half

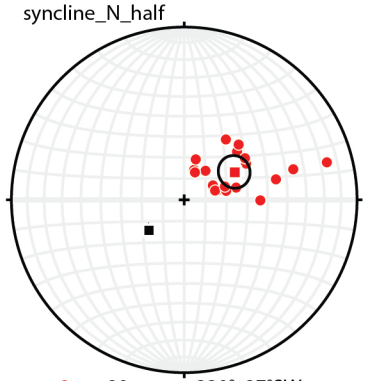

● n=20, m.v. = 330°, 27°SW
Mississippian-Pennsylvanian
▲ n=1, m.v. = 320°, 22°NE
Tertiary sediments

32. Haworth_E_limb_Pinto_Ck_syncline_N_half_rotated

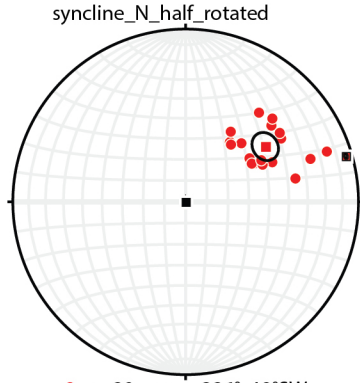

● n=20, m.v. = 326°, 49°SW
Mississippian-Pennsylvanian
Tertiary sediments horizontal

33. Haworth_E_limb_E_anticline

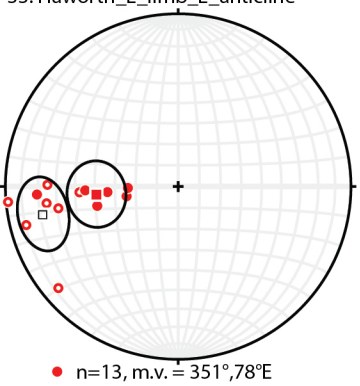

n=13, m.v. = 351°,78°E
Mississippian-Pennsylvanian

34. Haworth_W_limb_W_syncline

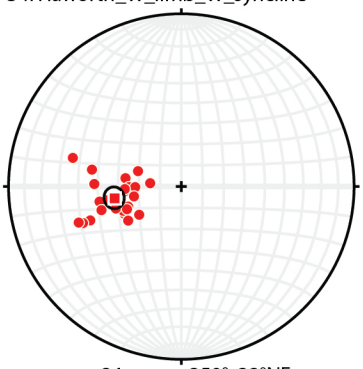

n=24, m.v. = 350°, 32°NE
Mississippian

35. Haworth_E_limb_W_syncline

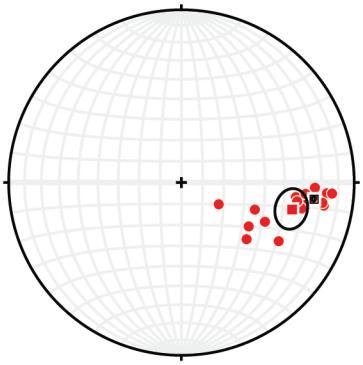

n=17, m.v. = 013°, 58°NW
Mississippian

36. Haworth_W_limb_Pinto_Ck_
syncline_S_half

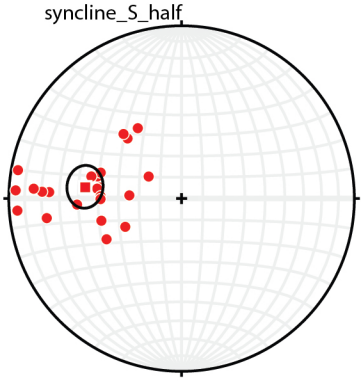

n=24, m.v. = 007°, 47°E
Miss-Penn-Cretaceous

37. Haworth_E_limb_Pinto_Ck_
syncline_S_half

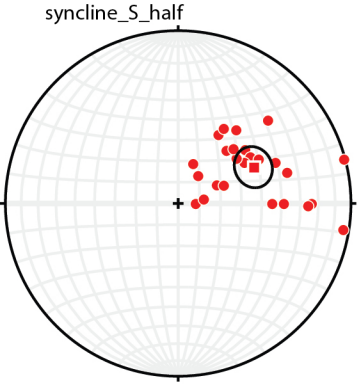

n=25, m.v. = 334°, 40°SW
Miss-Penn-Cretaceous

38. Larsen_Riva_W_limb_Pinto_Ck_
syncline_N_half

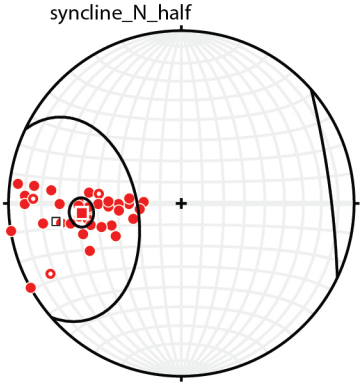

n=41, m.v. = 355°, 53°E
Mississippian-Permian

39. Larsen_Riva_E_limb_Pinto_Ck_
syncline_N_half

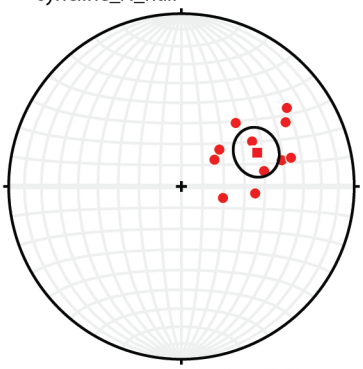

n=11, m.v. = 335°, 39°SW
Mississippian-Permian

40. Larsen_Riva_W_limb_W_anticline

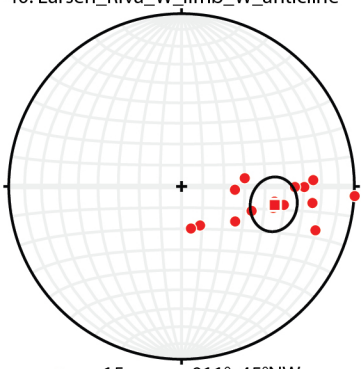

n=15, m.v. = 011°, 45°NW
Mississippian

41. Larsen_Riva_W_limb_E_syncline

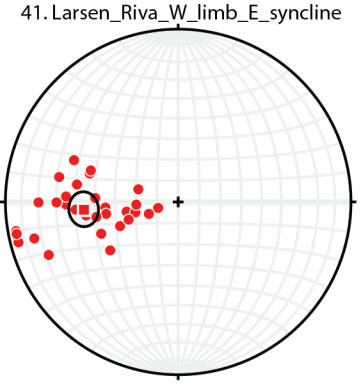

n=31, m.v. = 356°, 46°E
Permian-Cretaceous

42. Larsen_Riva_E_limb_E_syncline

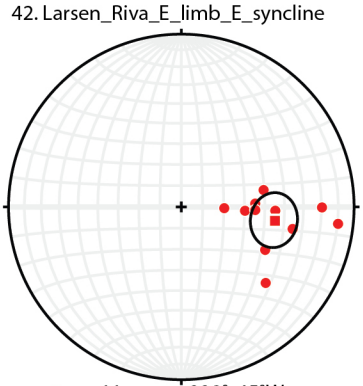

n=11, m.v. = 008°, 45°W
Permian-Cretaceous

43. Larsen_Riva_W_limb_Pinto_Ck_
syncline_S_half

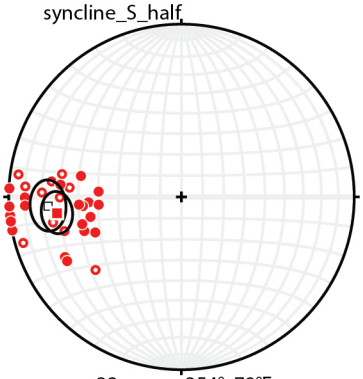

n=32, m.v. = 354°, 79°E
Devonian-Mississippian

44. Larsen_Riva_E_limb_Pinto_Ck_
syncline_S_half

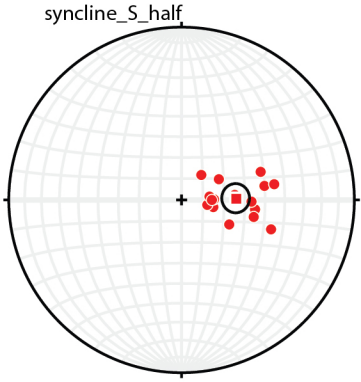

n=16, m.v. = 358°, 26°W
Mississippian-Cretaceous

45. Nolan_1971_W_limb_Pinto_Ck_
syncline_N_third

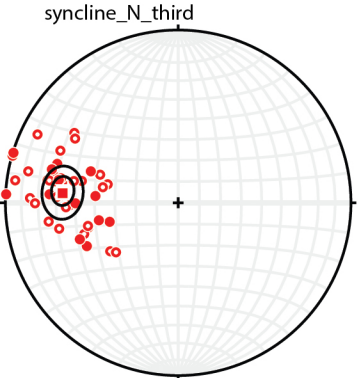

n=46, m.v. = 006°, 77°W
(overturned)
Silurian-Pennsylvanian

46. Nolan_1971_W_limb_Pinto_Ck_
syncline_middle_third

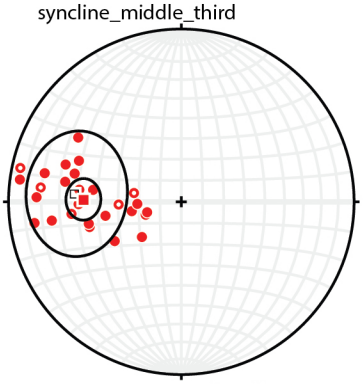

n=27, m.v. = 002°, 59°E
Mississippian-Pennsylvanian

47. Nolan_1971_W_limb_Pinto_Ck_
syncline_W_range_flank

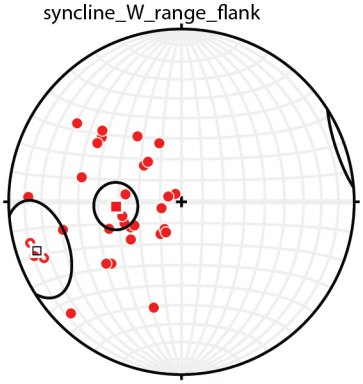

n=31, m.v. = 354°, 35°E
Cretaceous

48. Nolan_1971_E_limb_Pinto_Ck_
syncline_W_range_flank

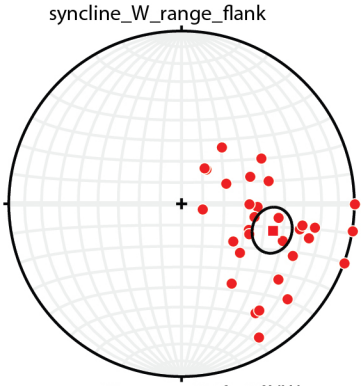

n=31, m.v. = 016°, 46°NW
Cretaceous

49. Nolan_1971_E_limb_Pinto_Ck_syncline_middle_third

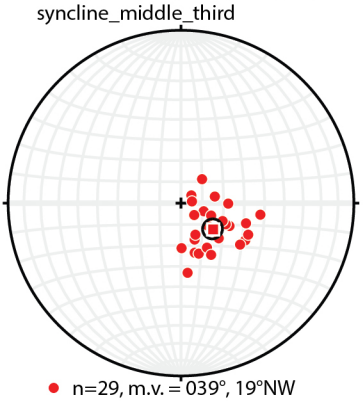

n=29, m.v. = 039°, 19°NW
Mississippian

50. Nolan_1971_E_limb_E_anticline_middle_third

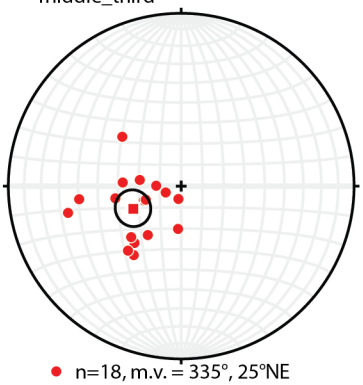

n=18, m.v. = 335°, 25°NE
Mississippian-Permian

51. Nolan_1971_E_limb_Pinto_Ck_snycline_S_third

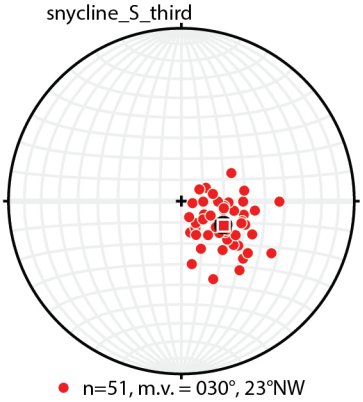

n=51, m.v. = 030°, 23°NW
Devonian-Pennsylvanian

52. Nolan_1971_1974_W_limb_Pinto_Ck_snycline_Newark_Canyon

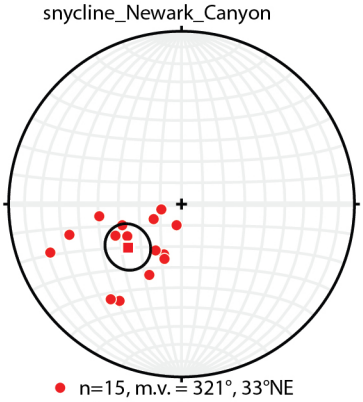

n=15, m.v. = 321°, 33°NE
Miss-Penn-Cretaceous
Late Eocene volcanics
approximately horizontal

53. Long_Nolan_1974_W_limb_Sentinel_Mtn_syncline_N

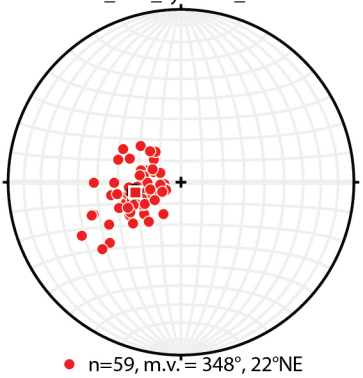

n=59, m.v. = 348°, 22°NE
Silurian-Devonian
Late Eocene volcanics
approximately horizontal

54. Long_E_limb_Sentinel_Mtn_syncline_N_half

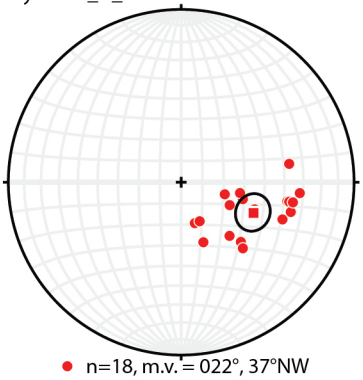

n=18, m.v. = 022°, 37°NW
Devonian
Late Eocene volcanics
approximately horizontal

55. Long_Nolan_1974_W_limb_Sentinel_Mtn_syncline_S_half

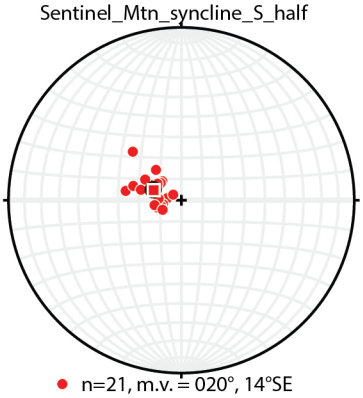

n=21, m.v. = 020°, 14°SE
Silurian-Devonian
Late Eocene volcanics
approximately horizontal

56. Long_E_limb_Sentinel_Mtn_syncline_S_half

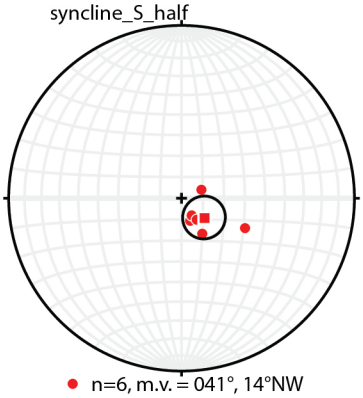

n=6, m.v. = 041°, 14°NW
Devonian
Late Eocene volcanics
approximately horizontal

57. Long_Nolan_1974_W_limb_Pinto_Ck_syncline_N

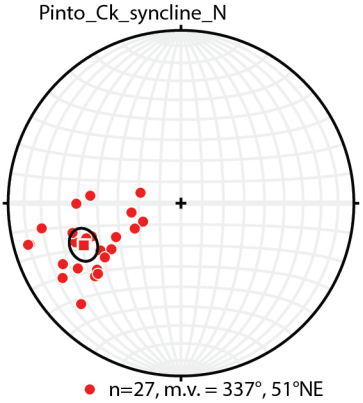

n=27, m.v. = 337°, 51°NE
Mississippian
Late Eocene volcanics
approximately horizontal

58. Long_Nolan_1974_E_limb_Pinto_Ck_syncline_N

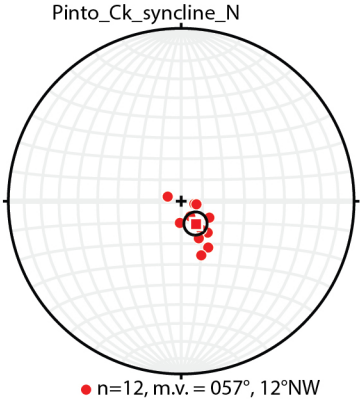

n=12, m.v. = 057°, 12°NW
Devonian-Mississippian
Late Eocene volcanics
approximately horizontal

59. Long_Nolan_1974_W_limb_Pinto_Ck_syncline_S

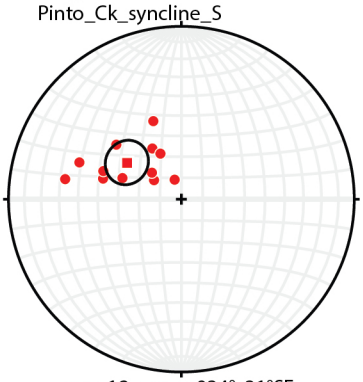

n=12, m.v. = 034°, 31°SE
Devonian-Mississippian
Late Eocene volcanics
approximately horizontal

60. Long_E_limb_Pinto_Ck_syncline_Alhambra_Hills

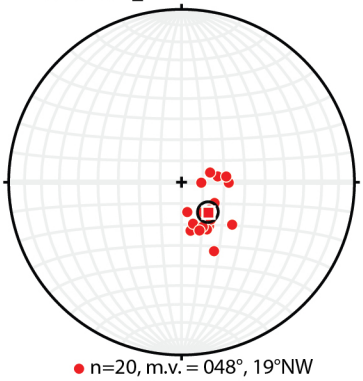

n=20, m.v. = 048°, 19°NW
Devonian
Late Eocene volcanics
approximately horizontal

61. Colgan_Millikan_S_Ruby_Mts

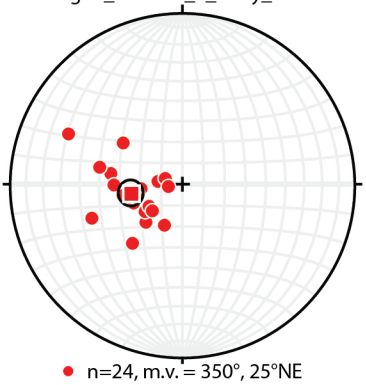

n=24, m.v. = 350°, 25°NE
Cambrian-Devonian

62. Nutt_Hart_NW_corner

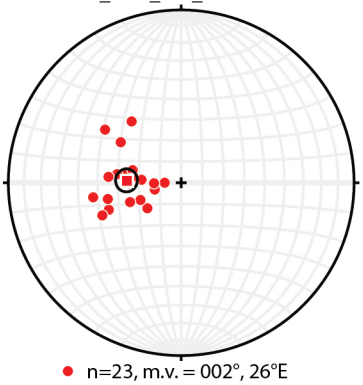

n=23, m.v. = 002°, 26°E
Cambrian-Ordovician

63. Nutt_Hart_N_central_W_limb_Illipah_anticline

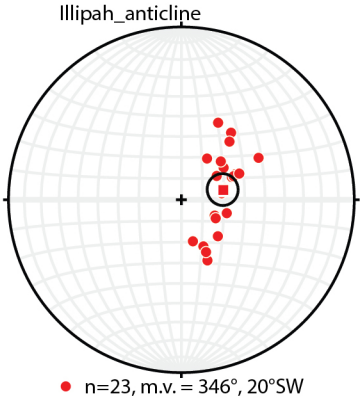

n=23, m.v. = 346°, 20°SW
Devonian

64. Nutt_Hart_NE_corner_E_limb_Illipah_anticline

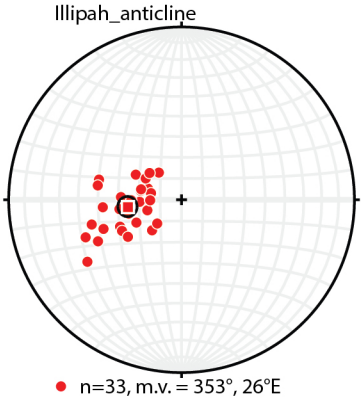

n=33, m.v. = 353°, 26°E
Devonian-Mississippian

65. Nutt_Hart_SE_quarter_E_limb_ Illipah_anticline

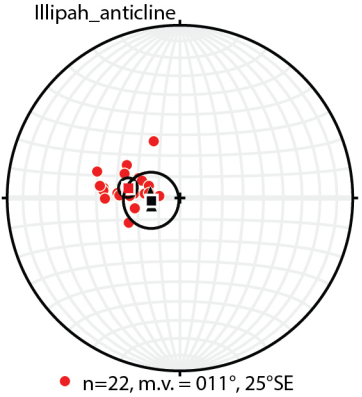

● n=22, m.v. = 011°, 25°SE
Devonian-Mississippian
▲ n=2, m.v. = 355°, 14°E
Tertiary sediments

66. Nutt_Hart_SE_quarter_E_limb_ Illipah_anticline_rotated

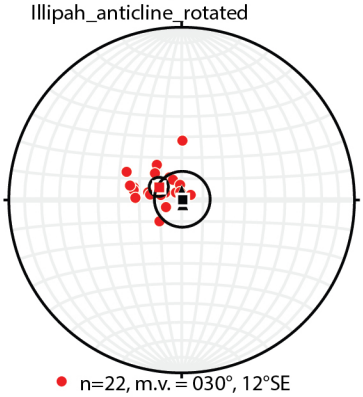

● n=22, m.v. = 030°, 12°SE
Devonian-Mississippian
Tertiary sediments horizontal

67. Nutt_Hart_SW_quarter

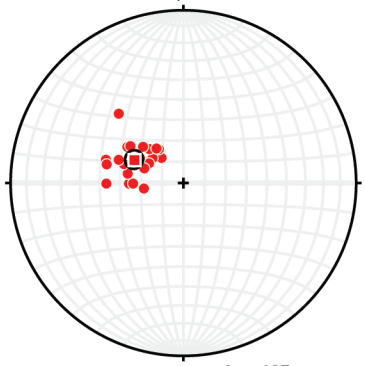

● n=22, m.v. = 025°, 26°SE
Cambrian-Devonian

68. Nutt_NW_corner

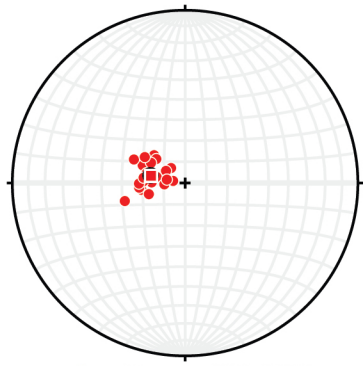

● n=22, m.v. = 025°, 26°SE
Cambrian-Devonian

69. Nutt_NW_central_W_limb_ Illipah_anticline

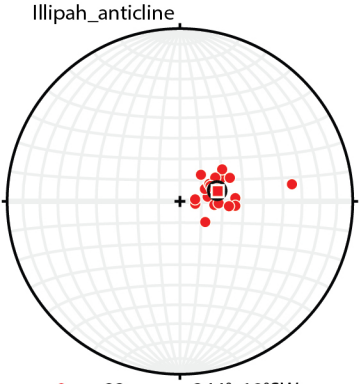

● n=23, m.v. = 344°, 18°SW
Ordovician-Mississippian

70. Nutt_NE_corner_W_limb_ Illipah_anticline

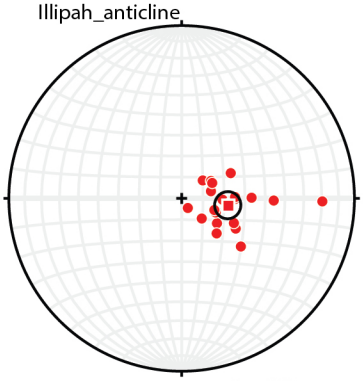

● n=22, m.v. = 358°, 22°W
Devonian-Mississippian

71. Nutt_NE_third_E_limb_ Illipah_anticline

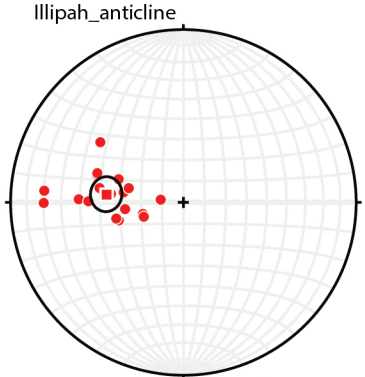

● n=18, m.v. = 006°, 37°E
Devonian-Mississippian

72. Nutt_E_central_third_E_limb_ Illipah_anticline

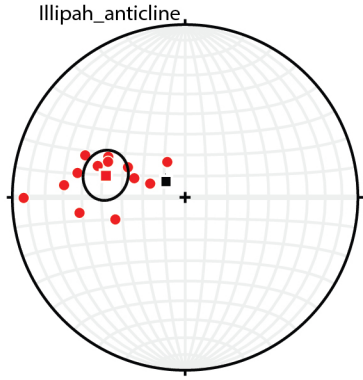

● n=14, m.v. = 016°, 40°E
Devonian-Mississippian
▲ n=1, m.v. = 040°, 12°E
Tertiary-Cretaceous

73. Nutt_E_central_third_E_limb_ Illipah_anticline_rotated

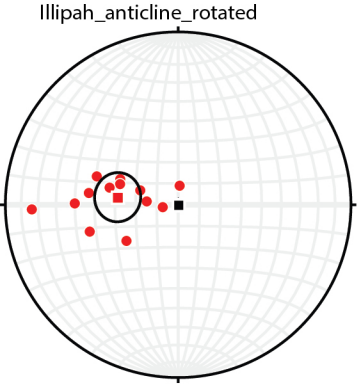

● n=14, m.v. = 016°, 30°E
Devonian-Mississippian
Tertiary-Cret. horizontal

74. Nutt_S_third_far_E_corner_E_ limb_Illipah_anticline

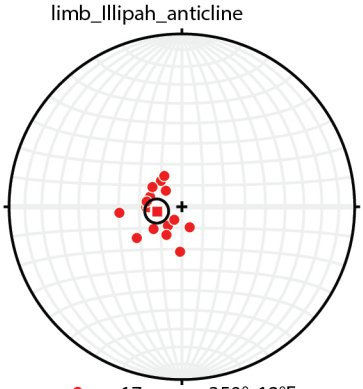

● n=17, m.v. = 350°, 12°E
Mississippian-Pennsylvanian

75. Nutt_SE_third_E_limb_Illipah_ anticline

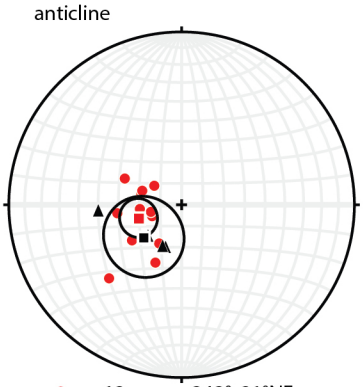

● n=12, m.v. = 343°, 21°NE
Devonian-Mississippian
▲ n=4, m.v. = 320°, 24°NE
Tertiary-Cretaceous

76. Nutt_SE_third_E_limb_Illipah_ anticline_rotated

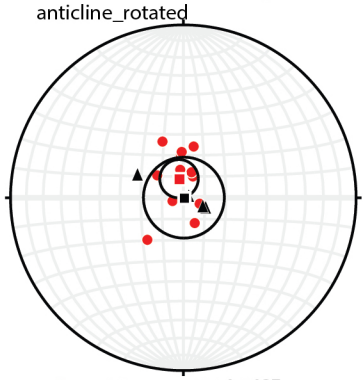

● n=12, m.v. = 077°, 9°SE
Devonian-Mississippian
Tertiary-Cret. horizontal

77. Nutt_S_central_W_limb_Illipah_ anticline

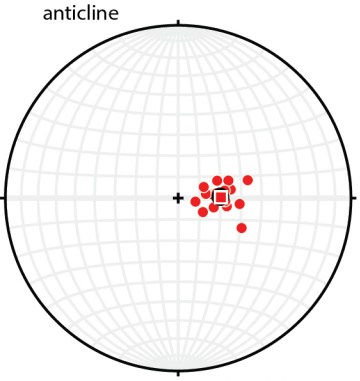

● n=19, m.v. = 358°, 20°W
Devonian-Mississippian

78. Nutt_SW_third_W_limb_Illipah_ anticline

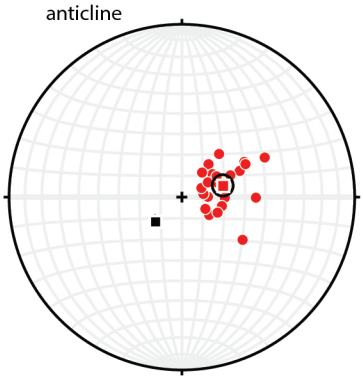

● n=23, m.v. = 344°, 21°SW
Mississippian-Pennsylvanian
▲ n=1, m.v. = 318°, 17°NE
Oligocene

79. Nutt_SW_third_W_limb_Illipah_ anticline_rotated

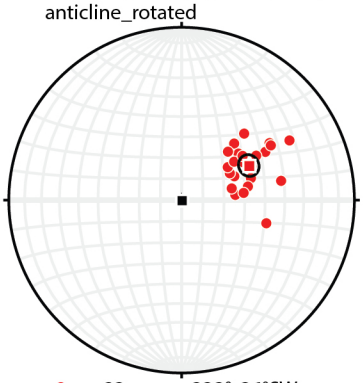

● n=23, m.v. = 333°, 36°SW
Mississippian-Pennsylvanian
Oligocene horizontal

80. Nutt_SW_corner_W_limb_Illipah_ anticline

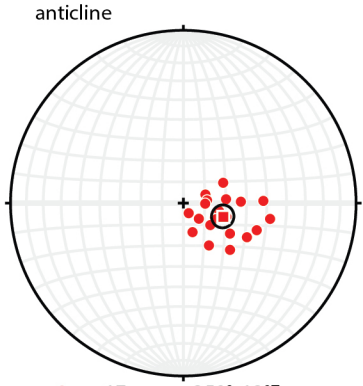

● n=17, m.v. = 350°, 12°E
Mississippian-Pennsylvanian

81. Campbell_Tomastik_W_limb_Buck_Mtn_syncline

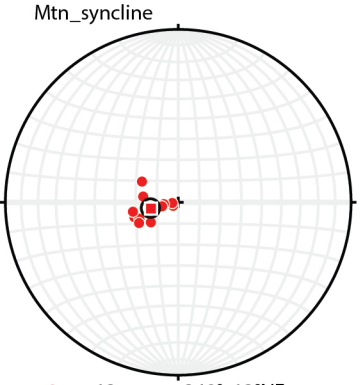

n=13, m.v. = 348°, 13°NE
Mississippian-Pennsylvanian

82. Connell_N_third

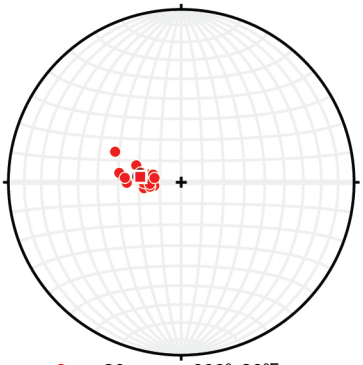

n=20, m.v. = 008°, 20°E
Pennsylvanian-Permian

83. Connell_middle_third

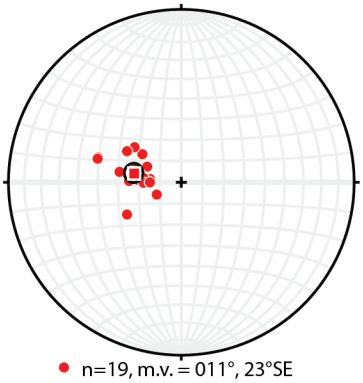

n=19, m.v. = 011°, 23°SE
Mississippian-Permian

84. Otto_N_quarter_W_limb_Butte_syncline

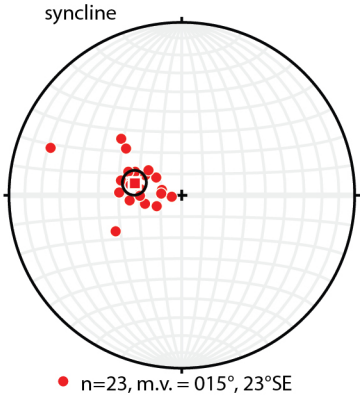

n=23, m.v. = 015°, 23°SE
Pennsylvanian-Permian

85. Otto_2nd_quarter_from_N_W_limb_Butte_syncline

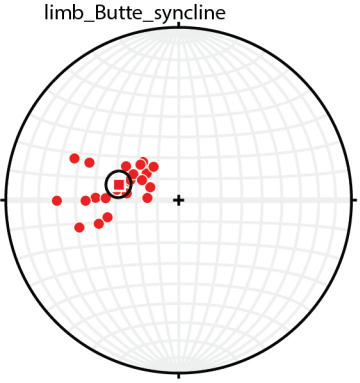

n=24, m.v. = 015°, 29°SE
Pennsylvanian-Permian

86. Otto_2nd_quarter_from_N_E_limb_Butte_syncline

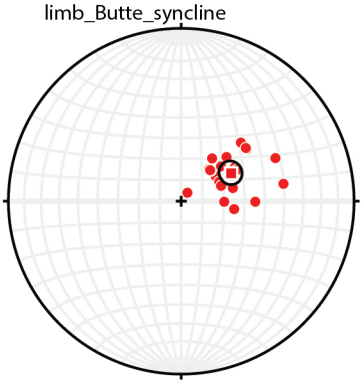

n=21, m.v. = 330°, 27°SW
Permian

87. Otto_2nd_quarter_from_S_W_limb_Butte_syncline

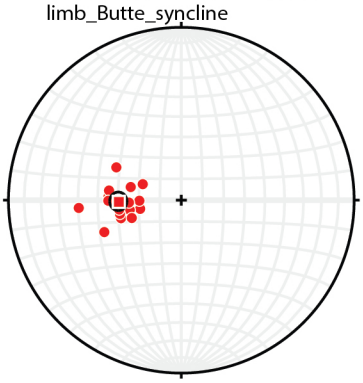

n=19, m.v. = 359°, 30°E
Pennsylvanian-Permian

88. Otto_2nd_quarter_from_S_E_limb_Butte_syncline

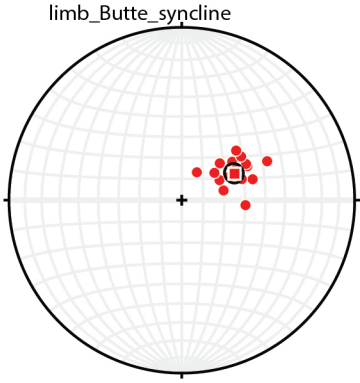

n=18, m.v. = 333°, 28°SW
Permian

89. Douglass_E_limb_Butte_syncline

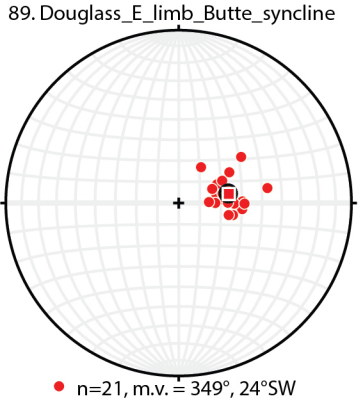

n=21, m.v. = 349°, 24°SW
Permian-Triassic

90. Douglass_W_limb_Butte_syncline

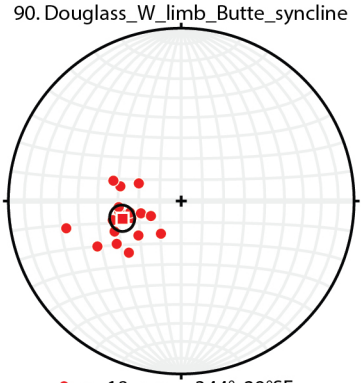

n=18, m.v. = 344°, 29°SE
Permian-Triassic

91. Douglass_E_limb_W_syncline

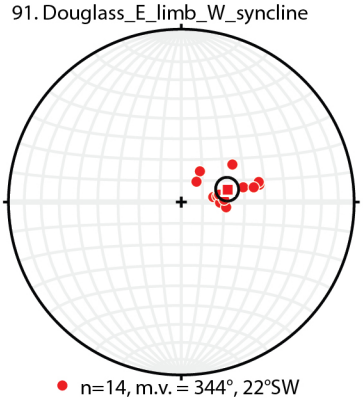

n=14, m.v. = 344°, 22°SW
Permian-Triassic

92. Douglass_W_limb_W_syncline

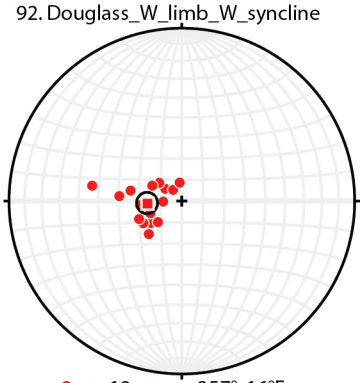

n=19, m.v. = 357°, 16°E
Permian

93. Douglass_E_limb_Butte_syncline

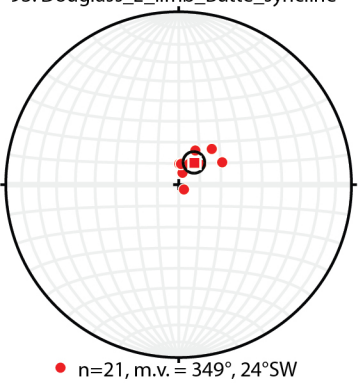

n=21, m.v. = 349°, 24°SW
Permian-Triassic

94. Fritz_N_third

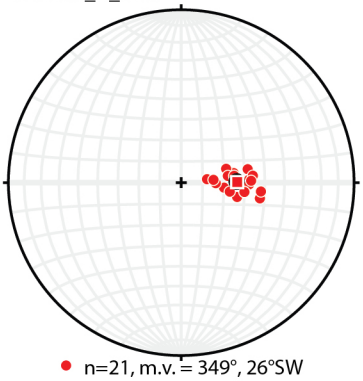

n=21, m.v. = 349°, 26°SW
Cambrian-Mississippian

95. Fritz_middle_third

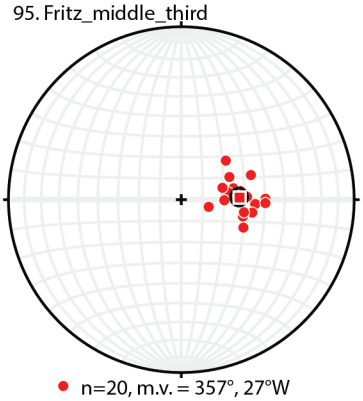

n=20, m.v. = 357°, 27°W
Cambrian-Pennsylvanian

96. Fritz_S_third

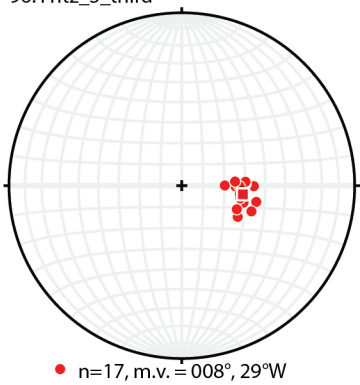

n=17, m.v. = 008°, 29°W
Ordovician-Mississippian

97. Pancake_Summit_W_half

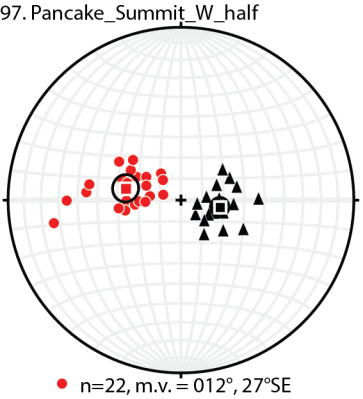

● n=22, m.v. = 012°, 27°SE
Mississippian-Pennsylvanian
▲ n=20, m.v. = 010°, 18°W
Late Eocene

98. Pancake_Summit_W_half_rotated

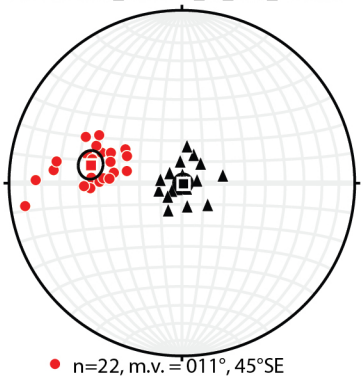

● n=22, m.v. = 011°, 45°SE
Mississippian-Pennsylvanian
Late Eocene horizontal

99. Pancake_Summit_E_half

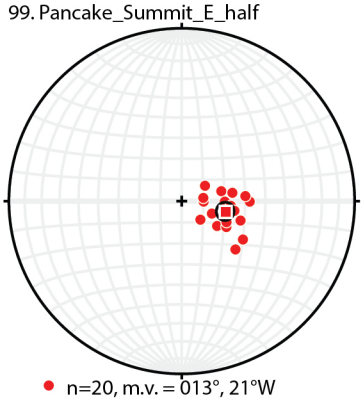

● n=20, m.v. = 013°, 21°W
Mississippian-Pennsylvanian

100. Nolan_1974_Pancake_Range_W_limb_Sentinel_Mtn_syncline

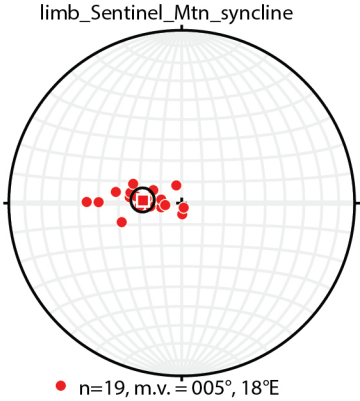

● n=19, m.v. = 005°, 18°E
Devonian-Mississippian
Late Eocene volcanics
approximately horizontal

101. Nolan_1974_Pancake_Range_E_limb_Sentinel_Mtn_syncline

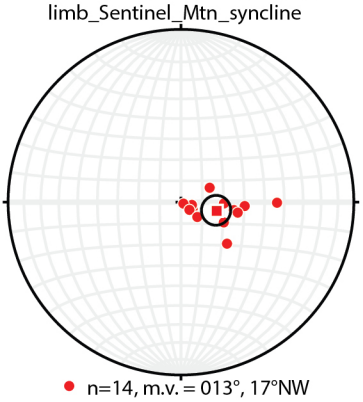

● n=14, m.v. = 013°, 17°NW
Devonian-Mississippian
Late Eocene volcanics
approximately horizontal

102. Nolan_1974_Pancake_Range_E_limb_Pinto_Ck_syncline

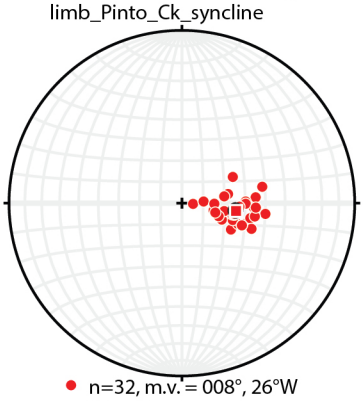

● n=32, m.v. = 008°, 26°W
Mississippian
Late Eocene volcanics
approximately horizontal

103. McDonald_W_limb_Sentinel_Mtn_syncline

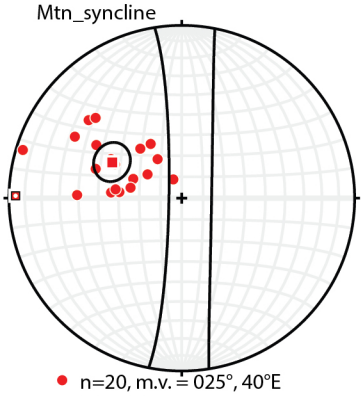

● n=20, m.v. = 025°, 40°E
Mississippian

104. McDonald_E_limb_Sentinel_Mtn_syncline_N_half

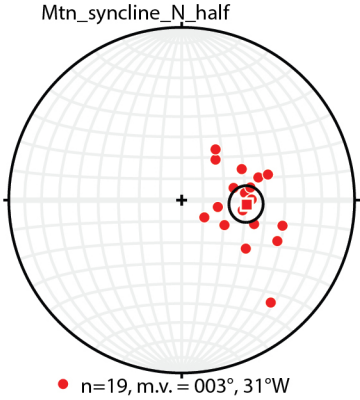

● n=19, m.v. = 003°, 31°W
Mississippian

105. McDonald_W_limb_Pinto_Ck_syncline_N

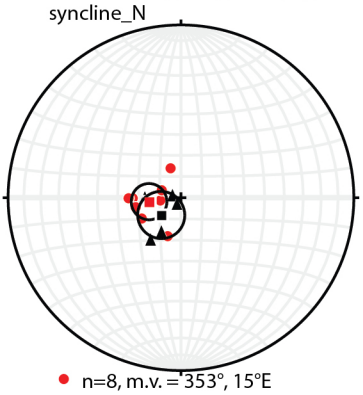

● n=8, m.v. = 353°, 15°E
Mississippian
▲ n=5, m.v. = 318°, 12°NE
Oligocene

106. McDonald_W_limb_Pinto_Ck_syncline_N_rotated

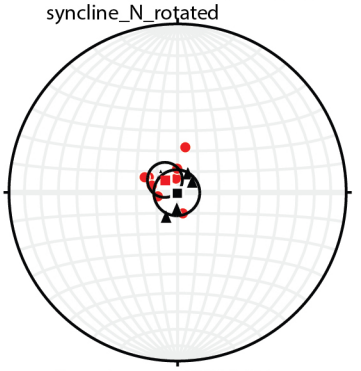

● n=8, m.v. = 045°, 9°SE
Mississippian
Oligocene horizontal

107. McDonald_E_limb_Pinto_Ck_syncline_N

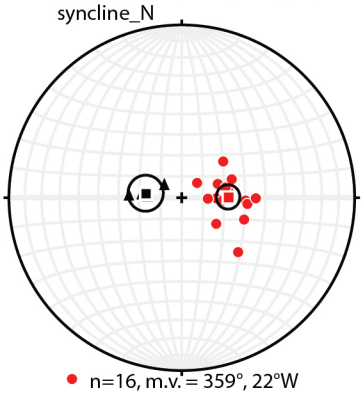

● n=16, m.v. = 359°, 22°W
Devonian-Mississippian
▲ n=4, m.v. = 007°, 17°E
Oligocene

108. McDonald_E_limb_Pinto_Ck_syncline_N_rotated

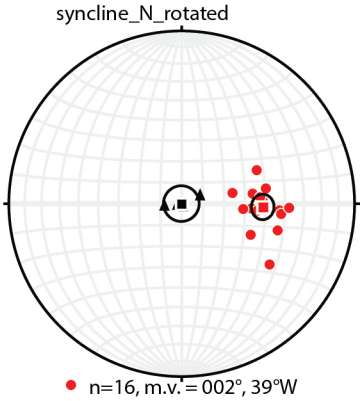

● n=16, m.v. = 002°, 39°W
Mississippian
Oligocene horizontal

109. McDonald_SW_quarter

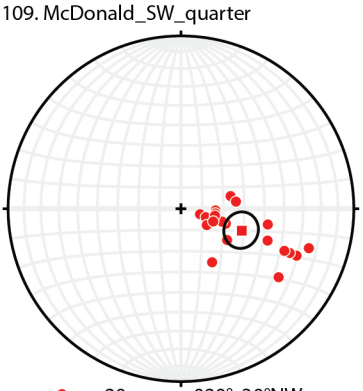

● n=20, m.v. = 020°, 30°NW
Mississippian

110. McDonald_SE_quarter

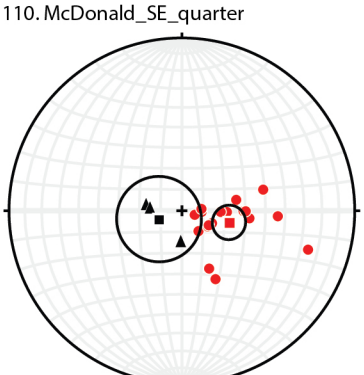

● n=18, m.v. = 014°, 23°NW
Devonian-Mississippian
▲ n=3, m.v. = 340°, 12°NE
Oligocene

111. McDonald_SE_quarter_rotated

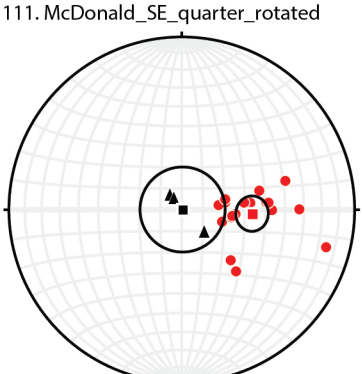

● n=18, m.v. = 003°, 33°W
Devonian-Mississippian
Oligocene horizontal

112. Hose_N_central

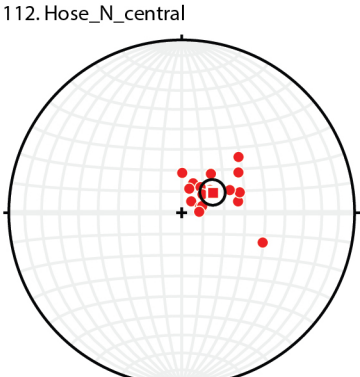

● n=18, m.v. = 327°, 17°SW
Silurian-Devonian

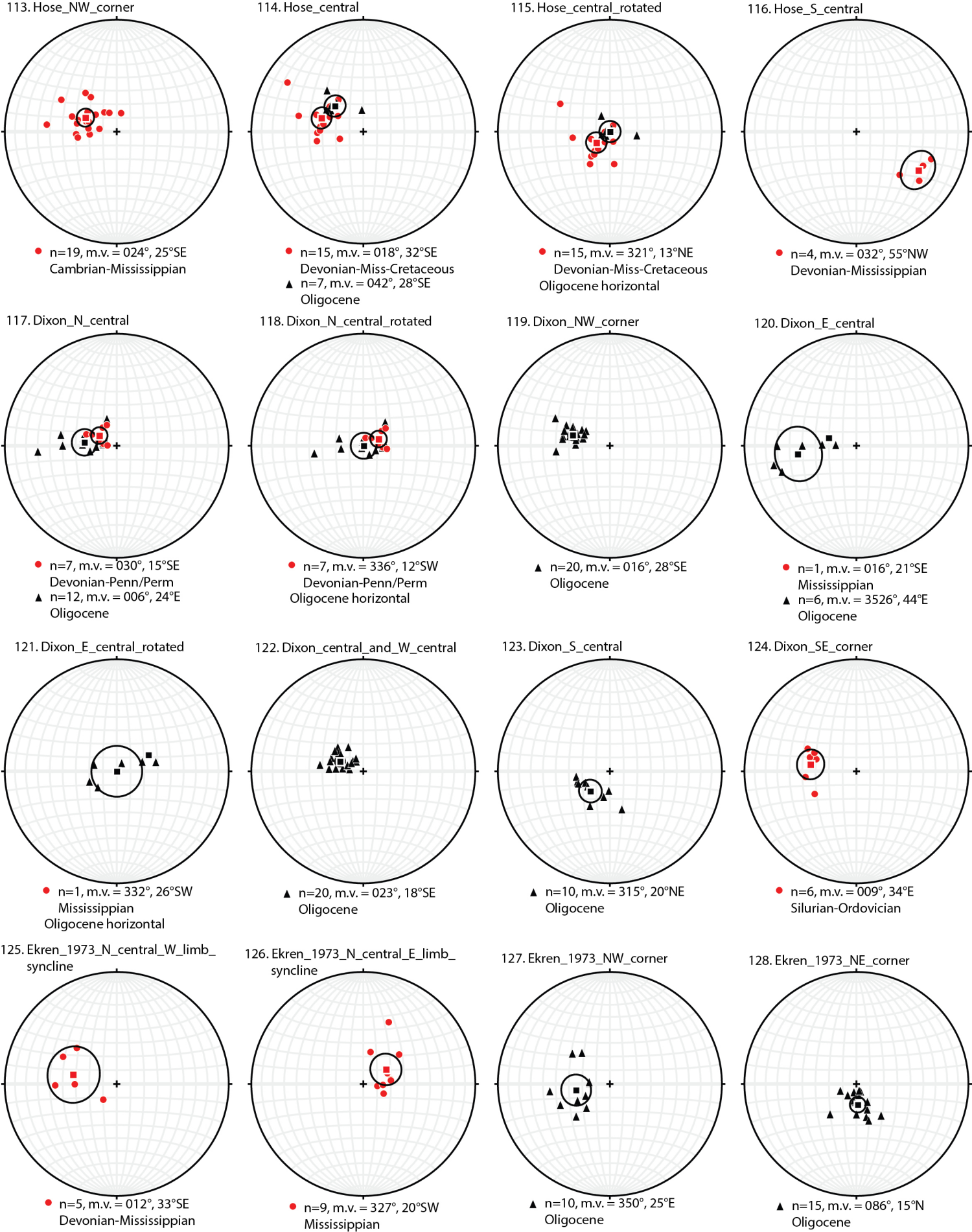
113. Hose_NW_corner
● n=19, m.v. = 024°, 25°SE
Cambrian-Mississippian
114. Hose_central
● n=15, m.v. = 018°, 32°SE
Devonian-Miss-Cretaceous
▲ n=7, m.v. = 042°, 28°SE
Oligocene
115. Hose_central_rotated
● n=15, m.v. = 321°, 13°NE
Devonian-Miss-Cretaceous
Oligocene horizontal
116. Hose_S_central
● n=4, m.v. = 032°, 55°NW
Devonian-Mississippian
117. Dixon_N_central
● n=7, m.v. = 030°, 15°SE
Devonian-Penn/Perm
▲ n=12, m.v. = 006°, 24°E
Oligocene
118. Dixon_N_central_rotated
● n=7, m.v. = 336°, 12°SW
Devonian-Penn/Perm
Oligocene horizontal
119. Dixon_NW_corner
▲ n=20, m.v. = 016°, 28°SE
Oligocene
120. Dixon_E_central
● n=1, m.v. = 016°, 21°SE
Mississippian
▲ n=6, m.v. = 3526°, 44°E
Oligocene
121. Dixon_E_central_rotated
● n=1, m.v. = 332°, 26°SW
Mississippian
Oligocene horizontal
122. Dixon_central_and_W_central
▲ n=20, m.v. = 023°, 18°SE
Oligocene
123. Dixon_S_central
▲ n=10, m.v. = 315°, 20°NE
Oligocene
124. Dixon_SE_corner
● n=6, m.v. = 009°, 34°E
Silurian-Ordovician
125. Ekren_1973_N_central_W_limb_ syncline
● n=5, m.v. = 012°, 33°SE
Devonian-Mississippian
126. Ekren_1973_N_central_E_limb_ syncline
● n=9, m.v. = 327°, 20°SW
Mississippian
127. Ekren_1973_NW_corner
▲ n=10, m.v. = 350°, 25°E
Oligocene
128. Ekren_1973_NE_corner
▲ n=15, m.v. = 086°, 15°N
Oligocene

129. Ekren_1973_center

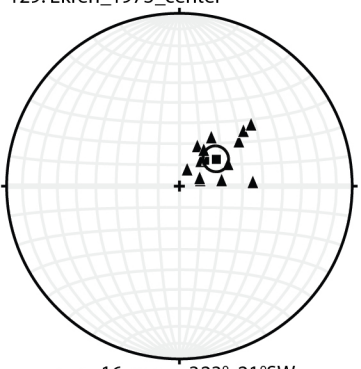

▲ n=16, m.v. = 323°, 21°SW
Oligocene

130. Ekren_1973_S_central_W_dips

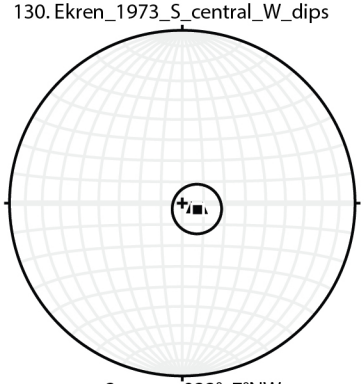

▲ n=2, m.v. = 022°, 7°NW
Oligocene

131. Ekren_1973_S_central_E_dips

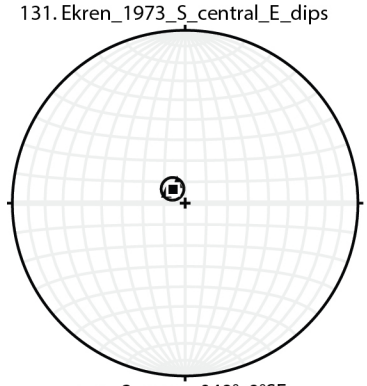

▲ n=3, m.v. = 049°, 9°SE
Oligocene

132. Quinlivan_W_of_N_central

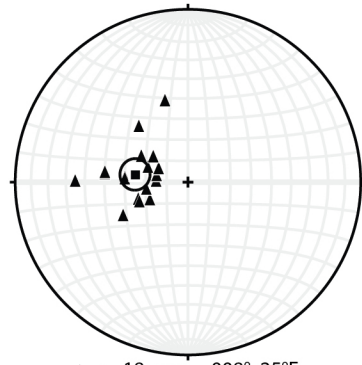

▲ n=18, m.v. = 008°, 25°E
Oligocene

133. Quinlivan_SW_quarter

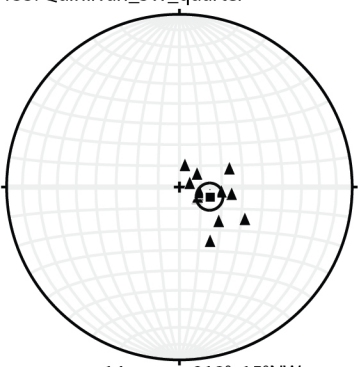

▲ n=14, m.v. = 018°, 15°NW
Oligocene

134. Quinlivan_NE_corner

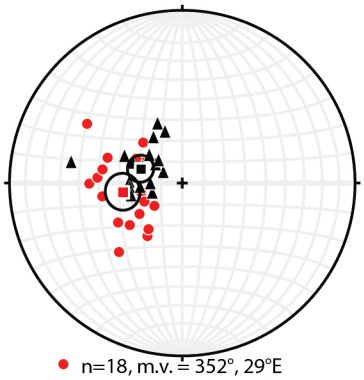

● n=18, m.v. = 352°, 29°E
Devonian-Mississippian
▲ n=18, m.v. = 019°, 21°SE
Oligocene

135. Quinlivan_NE_corner_rotated

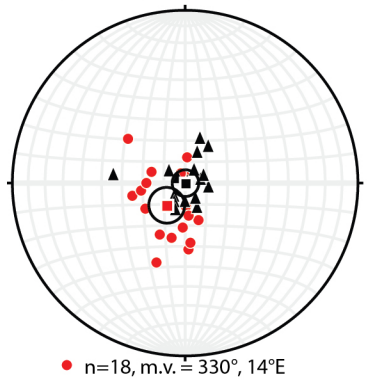

● n=18, m.v. = 330°, 14°E
Devonian-Mississippian
Oligocene horizontal

136. Quinlivan_E_of_N_central

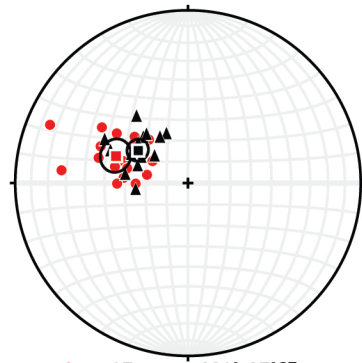

● n=17, m.v. = 021°, 37°SE
Devonian-Mississippian
▲ n=16, m.v. = 033°, 28°SE
Oligocene

137. Quinlivan_E_of_N_central_rotated

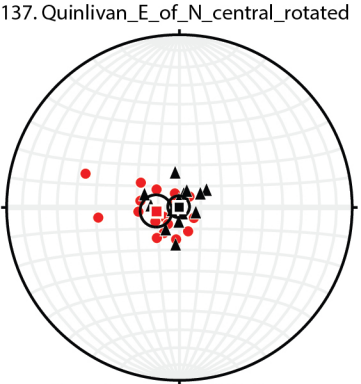

● n=17, m.v. = 352°, 11°E
Devonian-Mississippian
Oligocene horizontal

138. Quinlivan_S_central

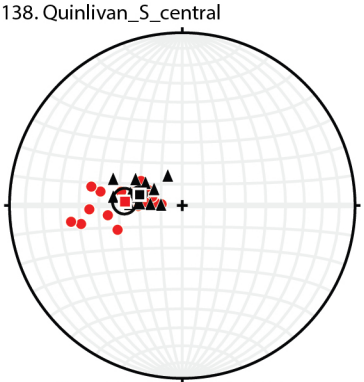

● n=20, m.v. = 004°, 27°E
Ordovician-Devonian
▲ n=20, m.v. = 015°, 21°SE
Oligocene

139. Quinlivan_S_central_rotated

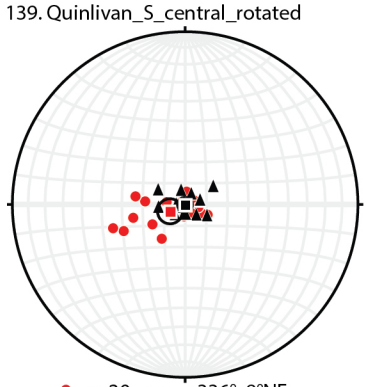

● n=20, m.v. = 336°, 8°NE
Ordovician-Devonian
Oligocene horizontal

140. Ekren_1972_N_central

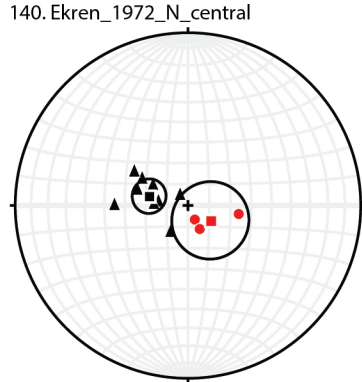

● n=3, m.v. = 034°, 13°NW
Devonian
▲ n=9, m.v. = 014°, 19°SE
Oligocene

141. Ekren_1972_N_central_rotated

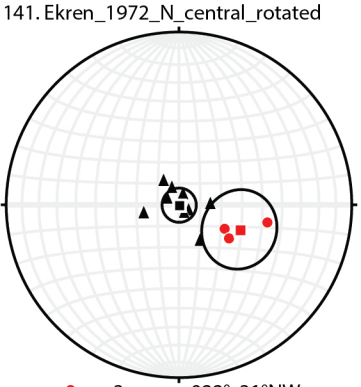

● n=3, m.v. = 022°, 31°NW
Devonian
Oligocene horizontal

142. Ekren_1972_SW_corner_SE_dips

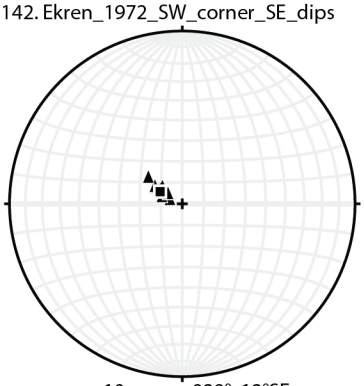

▲ n=10, m.v. = 029°, 12°SE
Oligocene

143. Ekren_1972_SW_corner_NW_dips

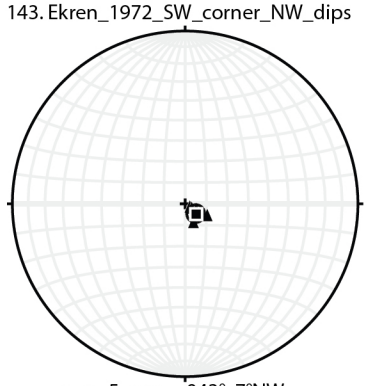

▲ n=5, m.v. = 043°, 7°NW
Oligocene

144. Martin_Naumann_SW_corner

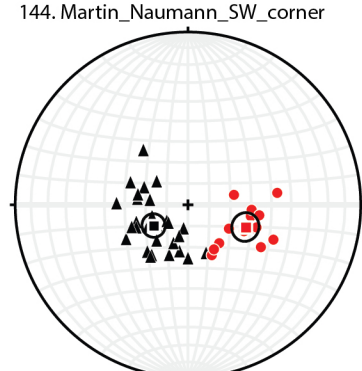

● n=14, m.v. = 021°, 29°NW
Ordovician-Mississippian
▲ n=28, m.v. = 329°, 19°NE
Oligocene

145. Martin_Naumann_SW_corner_rotated

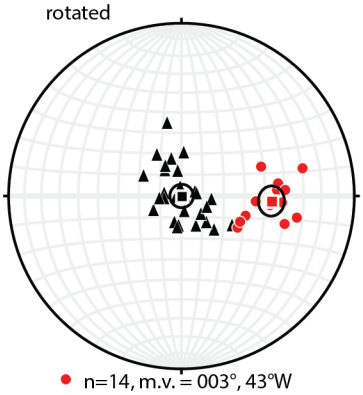

● n=14, m.v. = 003°, 43°W
Ordovician-Mississippian
Oligocene horizontal

146. Antelope_Mtn_W_quarter

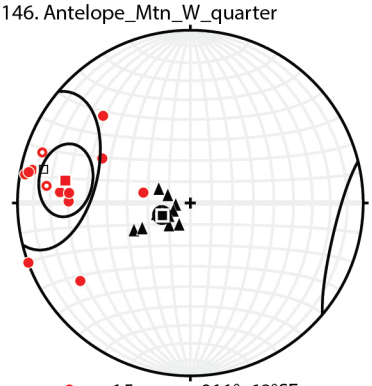

● n=15, m.v. = 011°, 68°SE
Pennsylvanian
▲ n=14, m.v. = 337°, 14°NE
Oligocene

147. Antelope_Mtn_W_quarter_rotated

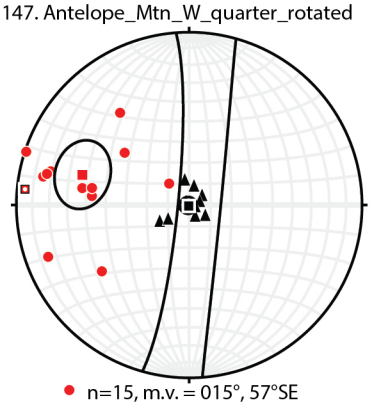

● n=15, m.v. = 015°, 57°SE
Pennsylvanian
Oligocene horizontal

148. Antelope_Mtn_W_limb_Illipah_anticline

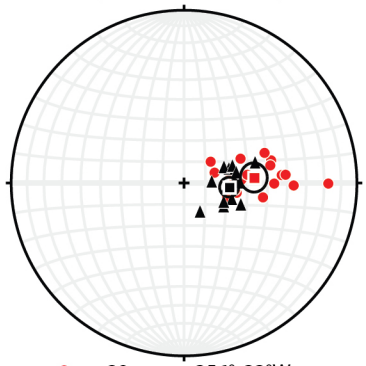

● n=20, m.v. = 356°, 33°W
Mississippian
▲ n=15, m.v. = 005°, 21°W
Oligocene

149. Antelope_Mtn_W_limb_Illipah_anticline_rotated

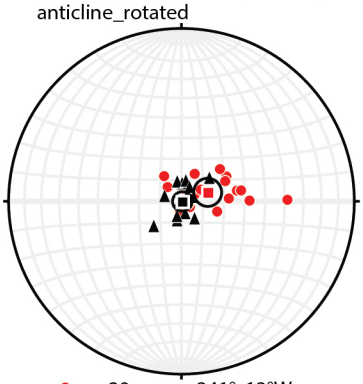

● n=20, m.v. = 341°, 13°W
Mississippian
Oligocene horizontal

150. Antelope_Mtn_E_limb_Illipah_anticline

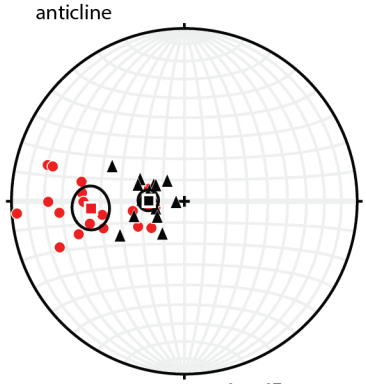

● n=20, m.v. = 356°, 45°E
Mississippian
▲ n=15, m.v. = 002°, 17°E
Oligocene

151. Antelope_Mtn_E_limb_Illipah_anticline_rotated

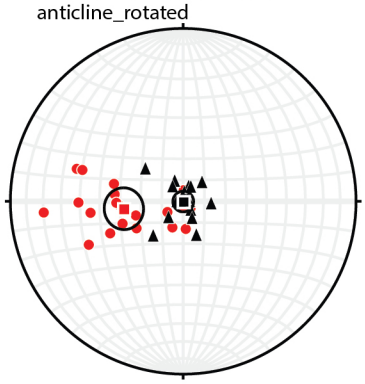

● n=20, m.v. = 353°, 28°E
Mississippian
Oligocene horizontal

152. Humphrey_N_third_far_W_end

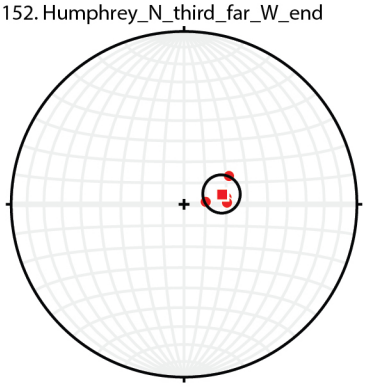

● n=4, m.v. = 345°, 18°SW
Silurian-Devonian

153. Humphrey_N_third_W_limb_Emigrant_anticline

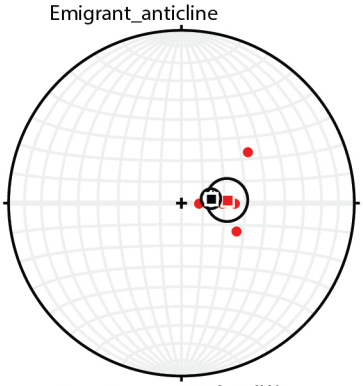

● n=7, m.v. = 356°, 22°W
Mississippian
▲ n=2, m.v. = 351°, 14°W
Cretaceous(?)

154. Humphrey_N_third_W_limb_Emigrant_anticline_rotated

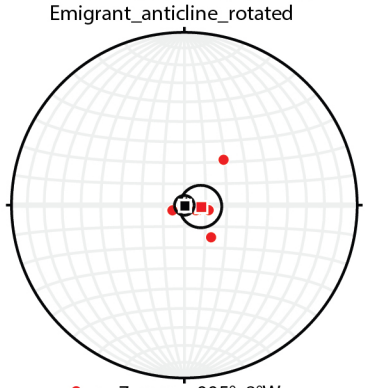

● n=7, m.v. = 005°, 8°W
Mississippian
Cretaceous(?) horizontal

155. Humphrey_N_third_W_limb_Little_Antelope_syncline

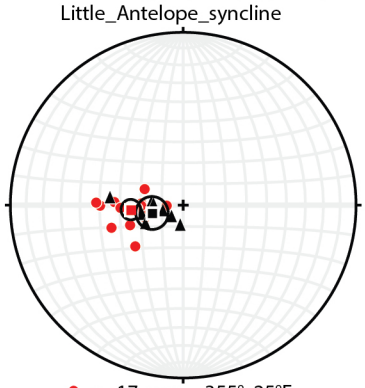

● n=17, m.v. = 355°, 25°E
Mississippian-Pennsylvanian
▲ n=8, m.v. = 346°, 15°E
Cretaceous(?)

156. Humphrey_N_third_W_limb_Little_Antelope_syncline_rotated

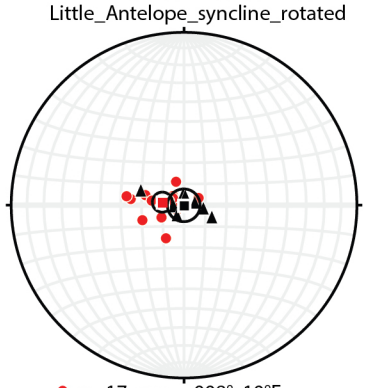

● n=17, m.v. = 008°, 10°E
Mississippian-Pennsylvanian
Cretaceous(?) horizontal

157. Humphrey_N_third_E_limb_Little_Antelope_syncline

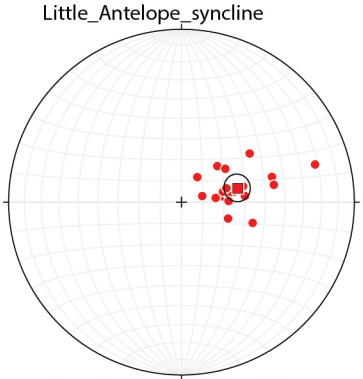

● n=20, m.v. = 346°, 27°W
Mississippian-Pennsylvanian

158. Humphrey_N_third_W_limb_Harris_syncline

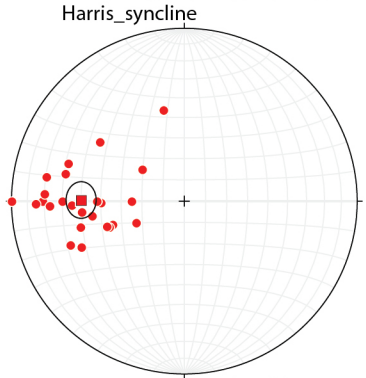

● n=27, m.v. = 001°, 50°E
Mississippian-Pennsylvanian

159. Humphrey_N_third_W_limb_Illipah_anticline

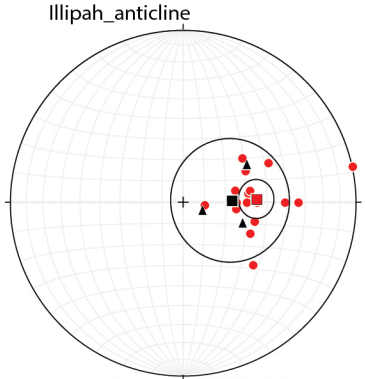

● n=17, m.v. = 356°, 35°W
Mississippian-Pennsylvanian
▲ n=3, m.v. = 358°, 23°W
Eocene

160. Humphrey_N_third_W_limb_Illipah_anticline_rotated

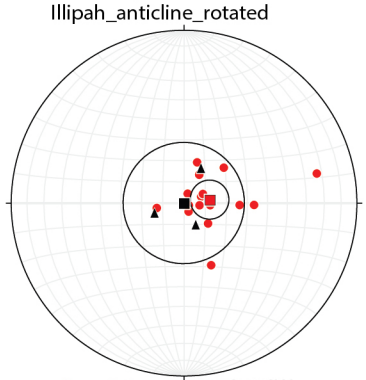

● n=17, m.v. = 352°, 12°W
Mississippian-Pennsylvanian
Eocene horizontal

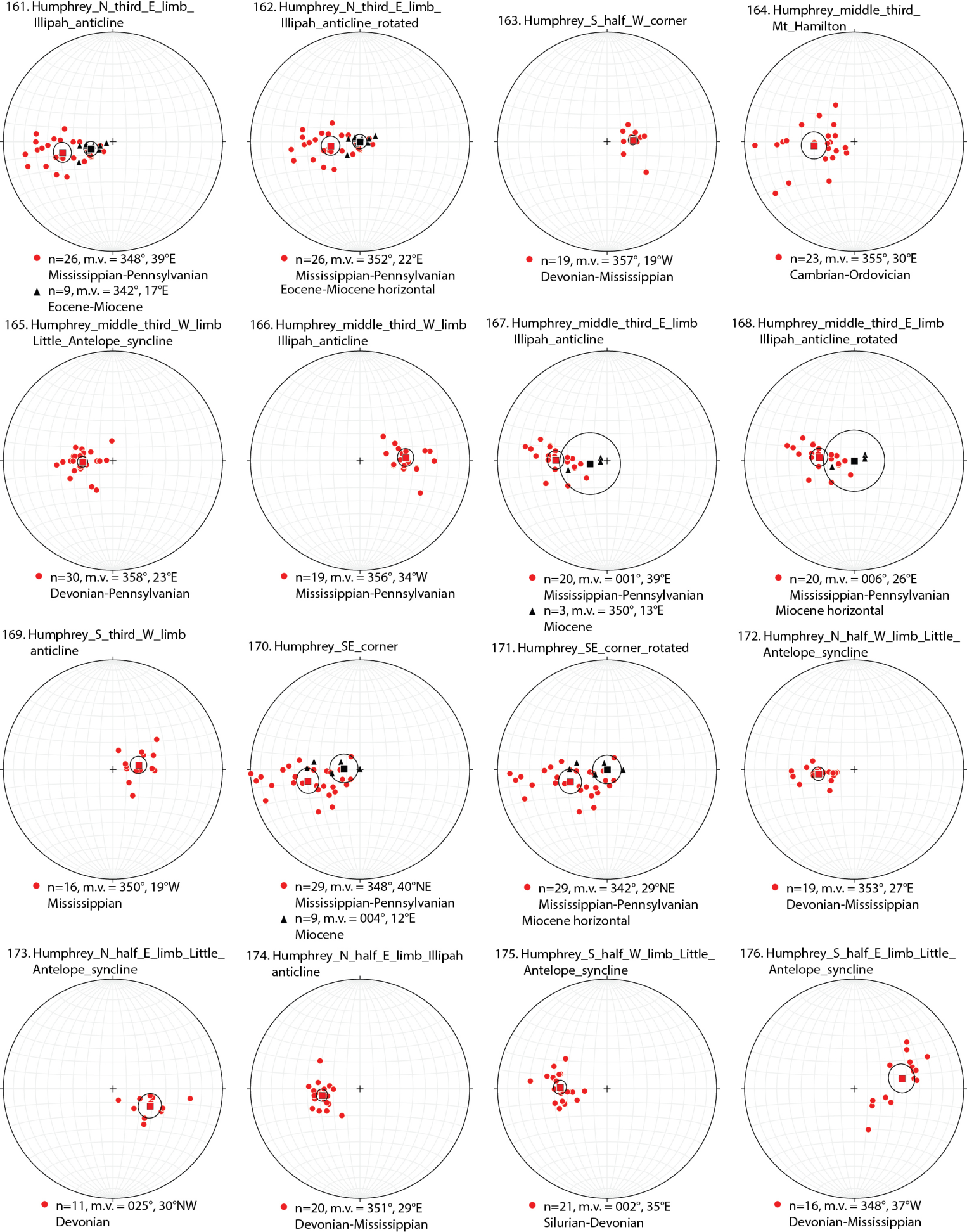
161. Humphrey_N_third_E_limb_ Illipah_anticline
n=26, m.v. = 348°, 39°E
Mississippian-Pennsylvanian
n=9, m.v. = 342°, 17°E
Eocene-Miocene
162. Humphrey_N_third_E_limb_ Illipah_anticline_rotated
n=26, m.v. = 352°, 22°E
Mississippian-Pennsylvanian
Eocene-Miocene horizontal
163. Humphrey_S_half_W_corner
n=19, m.v. = 357°, 19°W
Devonian-Mississippian
164. Humphrey_middle_third_ Mt_Hamilton
n=23, m.v. = 355°, 30°E
Cambrian-Ordovician
165. Humphrey_middle_third_W_limb Little_Antelope_syncline
n=30, m.v. = 358°, 23°E
Devonian-Pennsylvanian
166. Humphrey_middle_third_W_limb Illipah_anticline
n=19, m.v. = 356°, 34°W
Mississippian-Pennsylvanian
167. Humphrey_middle_third_E_limb Illipah_anticline
n=20, m.v. = 001°, 39°E
Mississippian-Pennsylvanian
n=3, m.v. = 350°, 13°E
Miocene
168. Humphrey_middle_third_E_limb Illipah_anticline_rotated
n=20, m.v. = 006°, 26°E
Mississippian-Pennsylvanian
Miocene horizontal
169. Humphrey_S_third_W_limb anticline
n=16, m.v. = 350°, 19°W
Mississippian
170. Humphrey_SE_corner
n=29, m.v. = 348°, 40°NE
Mississippian-Pennsylvanian
n=9, m.v. = 004°, 12°E
Miocene
171. Humphrey_SE_corner_rotated
n=29, m.v. = 342°, 29°NE
Mississippian-Pennsylvanian
Miocene horizontal
172. Humphrey_N_half_W_limb_Little_ Antelope_syncline
n=19, m.v. = 353°, 27°E
Devonian-Mississippian
173. Humphrey_N_half_E_limb_Little_ Antelope_syncline
n=11, m.v. = 025°, 30°NW
Devonian
174. Humphrey_N_half_E_limb_Illipah anticline
n=20, m.v. = 351°, 29°E
Devonian-Mississippian
175. Humphrey_S_half_W_limb_Little_ Antelope_syncline
n=21, m.v. = 002°, 35°E
Silurian-Devonian
176. Humphrey_S_half_E_limb_Little_ Antelope_syncline
n=16, m.v. = 348°, 37°W
Devonian-Mississippian

177. Humphrey_S_half_E_limb_Illipah_anticline

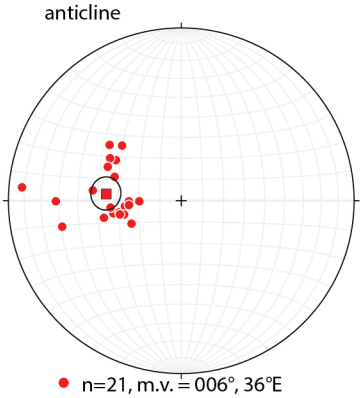

● n=21, m.v. = 006°, 36°E
Devonian-Mississippian

178. Tracy_SW_quarter

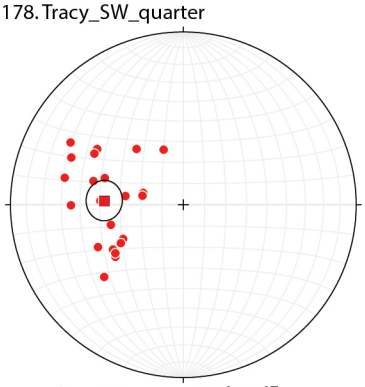

● n=22, m.v. = 003°, 38°E
Ordovician-Pennsylvanian

179. Tracy_SE_quarter

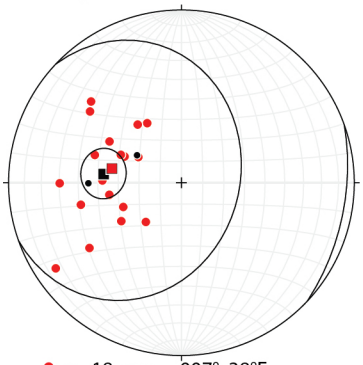

● n=18, m.v. = 007°, 38°E
Devonian-Pennsylvanian
▲ n=2, m.v. = 012°, 34°E
Oligocene

180. Tracy_SE_quarter_rotated

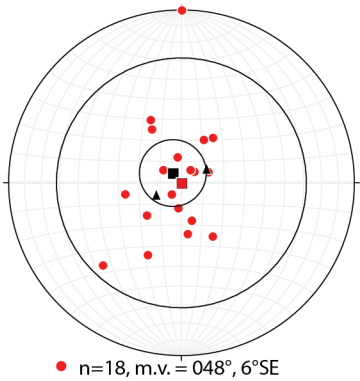

● n=18, m.v. = 048°, 6°SE
Devonian-Pennsylvanian
Oligocene horizontal

181. Moores_NW_corner

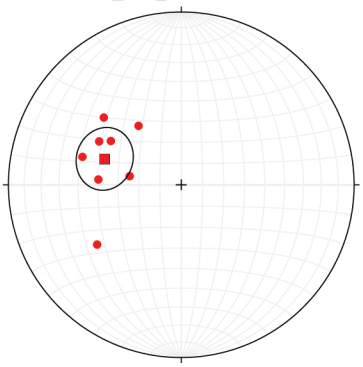

● n=8, m.v. = 019°, 39°E
Mississippian-Permian

182. Moores_N_central

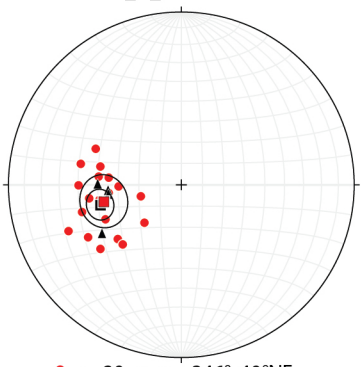

● n=20, m.v. = 346°, 40°NE
Ordovician-Pennsylvanian
▲ n=4, m.v. = 348°, 38°E
Oligocene

183. Moores_N_central_rotated

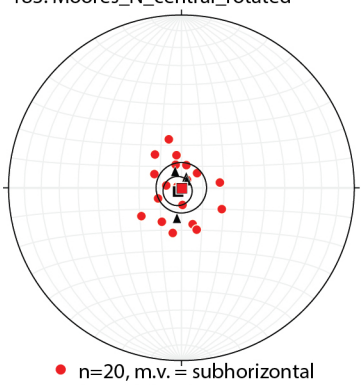

● n=20, m.v. = subhorizontal
Ordovician-Pennsylvanian
Oligocene horizontal

184. Moores_N_central_to_Currant_Summit_fault

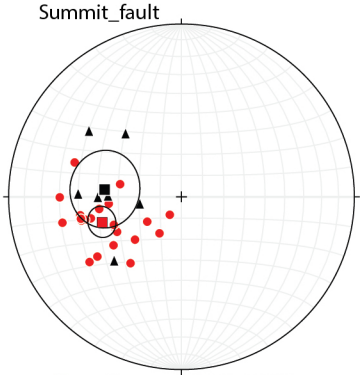

● n=23, m.v. = 343°, 40°NE
Cambrian-Pennsylvanian
▲ n=7, m.v. = 006°, 37°E
Oligocene

185. Moores_N_central_to_Currant_Summit_fault_rotated

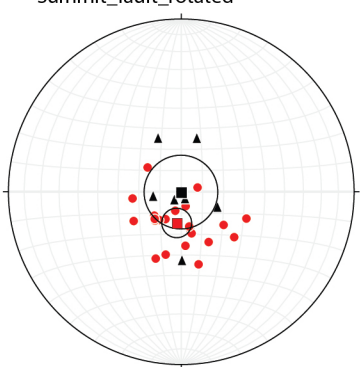

● n=23, m.v. = 278°, 15°N
Ordovician-Pennsylvanian
Oligocene horizontal

186. Moores_N_central_W_of_anticline_axis

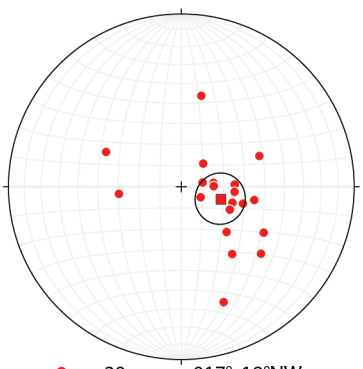

● n=20, m.v. = 017°, 19°NW
Cambrian

187. Moores_W_central_N_of_highway_6

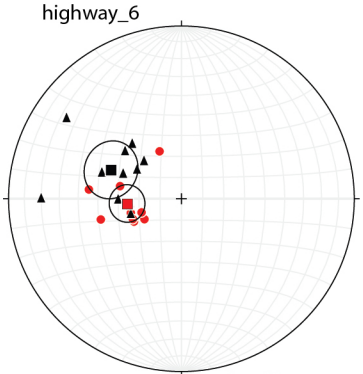

● n=10, m.v. = 355°, 26°E
Devonian-Mississippian
▲ n=10, m.v. = 022°, 36°E
Oligocene-Miocene

188. Moores_W_central_N_of_highway_6_rotated

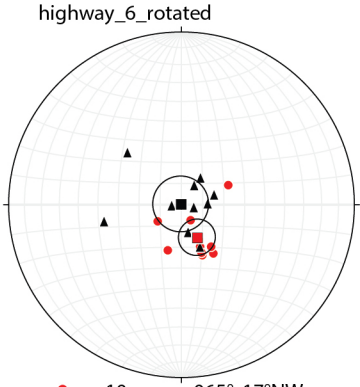

● n=10, m.v. = 065°, 17°NW
Devonian-Mississippian
Oligocene-Miocene horizontal

189. Moores_W_central_Horse_Camp_basin

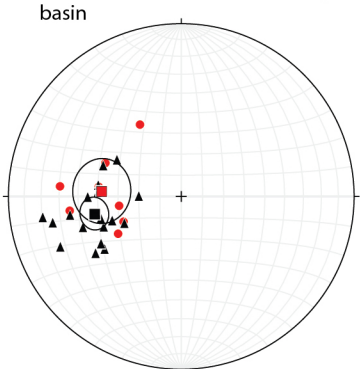

● n=8, m.v. = 004°, 38°E
Devonian-Mississippian
▲ n=20, m.v. = 349°, 43°NE
Oligocene-Miocene

190. Moores_W_central_Horse_Camp_basin

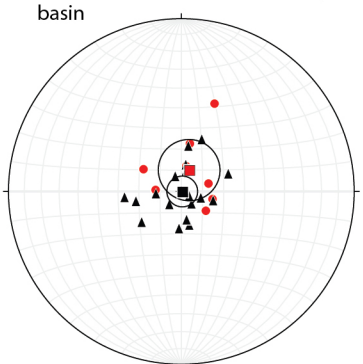

● n=8, m.v. = 290°, 11°SW
Devonian-Mississippian
Oligocene-Miocene horizontal

191. Moores_E_central_N_of_38_45'

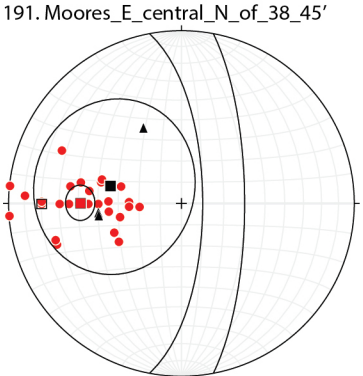

● n=28, m.v. = 000°, 51°E
Cambrian-Mississippian
▲ n=3, m.v. = 014°, 35°SE
Oligocene

192. Moores_E_central_N_of_38_45'_rotated

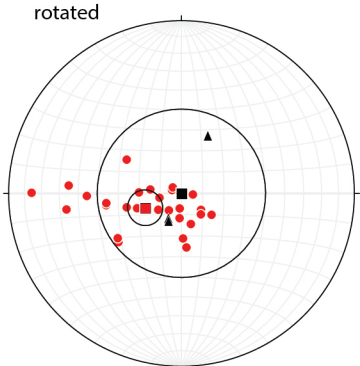

● n=28, m.v. = 339, 18°E
Cambrian-Mississippian
Oligocene horizontal

193. Moores_E_central_S_of_38_45'

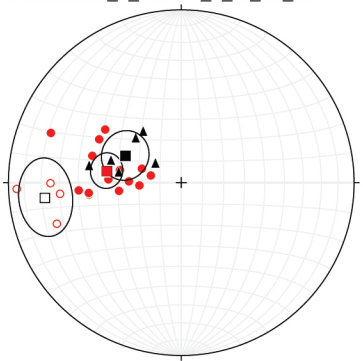

● n=20, m.v. = 004°, 52°E
Cambrian-Pennsylvanian
▲ n=6, m.v. = 026°, 30°SE
Oligocene

194. Moores_E_central_S_of_38_45'_rotated

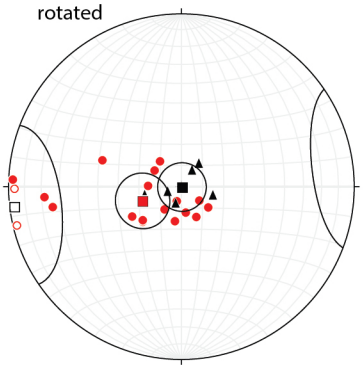

● n=20, m.v. = 004°, 52°E
Cambrian-Pennsylvanian
Oligocene horizontal

195. Moores_SW_corner

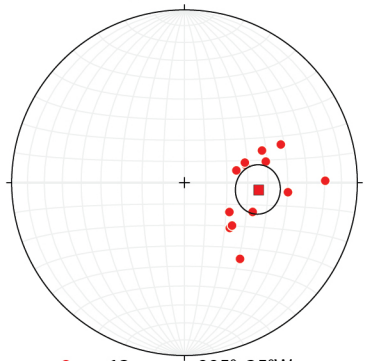

● n=13, m.v. = 005°, 35°W
Ordovician-Devonian

196. Moores_S_central

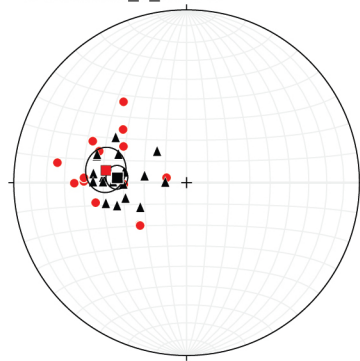

● n=15, m.v. = 009°, 39°E
Devonian-Mississippian
▲ n=19, m.v. = 005°, 33°E
Oligocene-Miocene

197. Moores_S_central_rotated

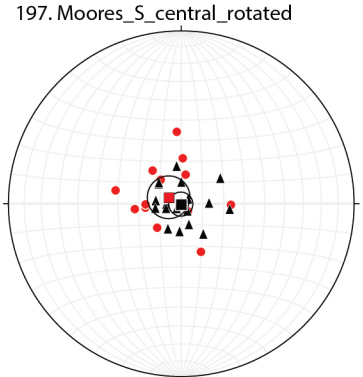

● n=15, m.v. = 027°, 7°E
Devonian-Mississippian
Oligocene-Miocene horizontal

198. Moores_SE_corner

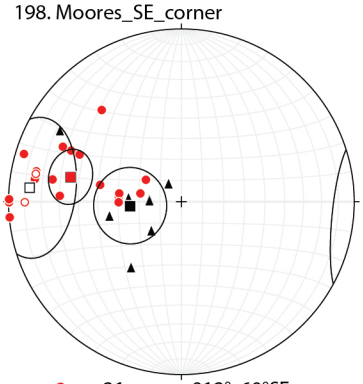

● n=21, m.v. = 012°, 60°SE
Ordovician-Pennsylvanian
▲ n=8, m.v. = 356°, 25°E
Oligocene

199. Moores_SE_corner_rotated

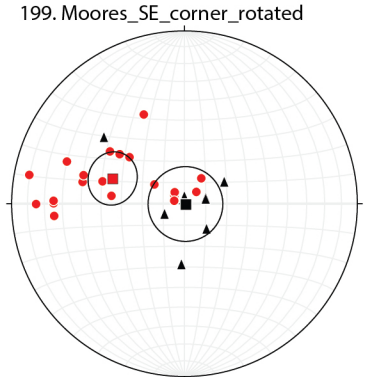

● n=21, m.v. = 019°, 36°SE
Ordovician-Pennsylvanian
Oligocene horizontal

200. Lund_1987_middle_third_W_of_anticline_axis

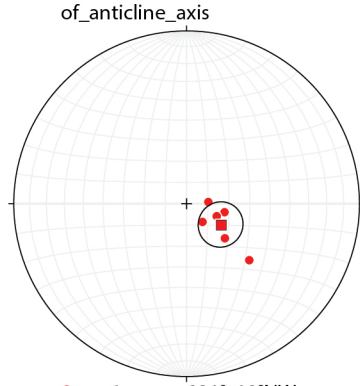

● n=6, m.v. = 031°, 19°NW
Ordovician-Mississippian

201. Lund_1987_S_third_E_of_anticline_axis

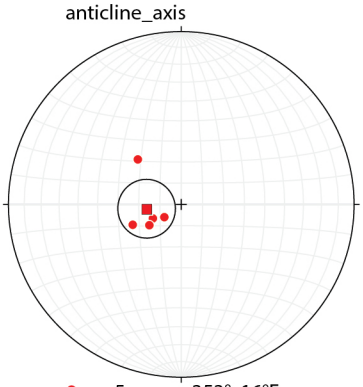

● n=5, m.v. = 353°, 16°E
Ordovician-Pennsylvanian

202. Lund_1988_N_half

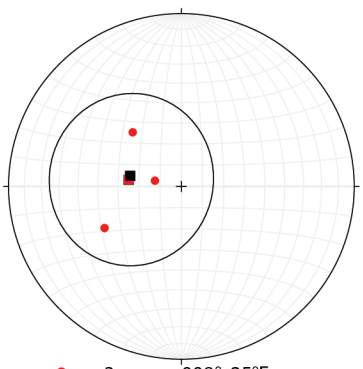

● n=3, m.v. = 008°, 25°E
Devonian-Pennsylvanian
▲ n=1, m.v. = 012°, 25°E
Oligocene

203. Lund_1988_N_half_rotated

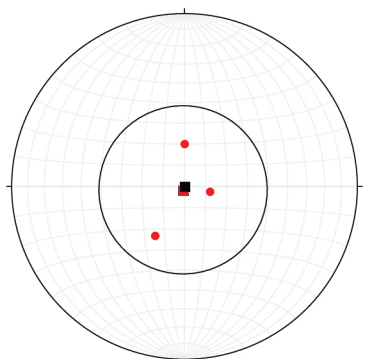

● n=3, m.v. = subhorizontal
Devonian-Pennsylvanian
Oligocene horizontal

204. Camilleri_S_Central

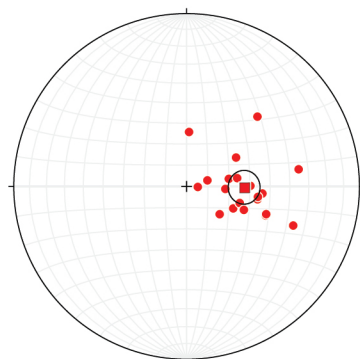

● n=20, m.v. = 001°, 27°W
Cambrian

205. Camilleri_SE_corner

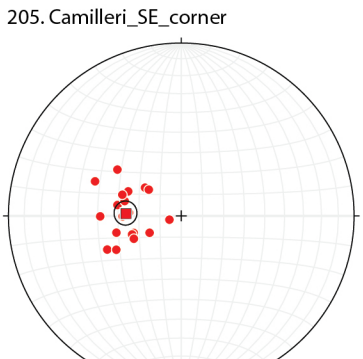

● n=20, m.v. = 003°, 26°E
Ordovician-Devonian

206. Lund_1988_S_half

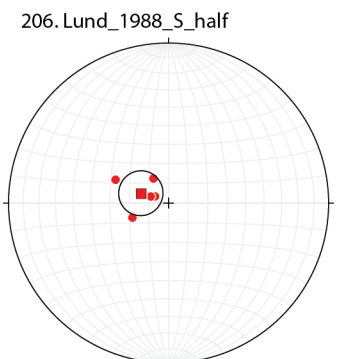

● n=5, m.v. = 020°, 15°SE
Devonian-Pennsylvanian

207. Fryxell_SW_quarter

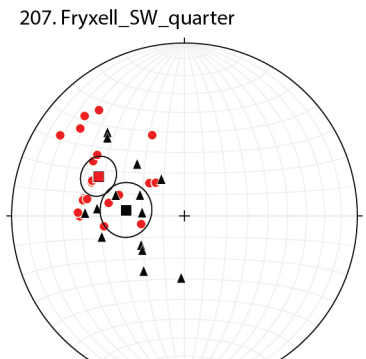

● n=20, m.v. = 025°, 46°SE
Cambrian-Ordovician
▲ n=14, m.v. = 006°, 28°E
Miocene

208. Fryxell_SW_quarter_rotated

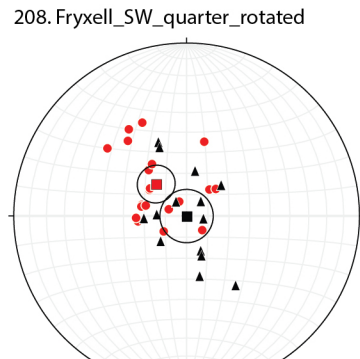

● n=20, m.v. = 046°, 21°SE
Cambrian-Ordovician
Miocene horizontal

209. Fryxell_NE_quarter_lower_limb_TMA

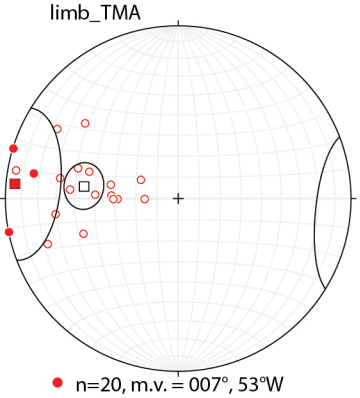

● n=20, m.v. = 007°, 53°W overturned)
Cambrian

210. Fryxell_SE_corner_upper_limb_TMA

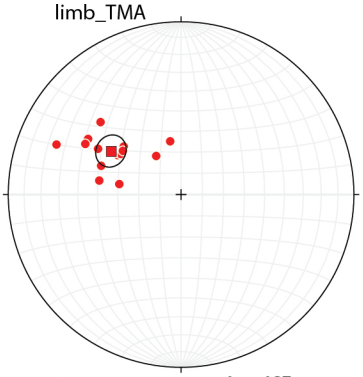

● n=15, m.v. = 032°, 40°SE
Cambrian-Ordovician

211. Bartley_Gleason_West_map_W_half

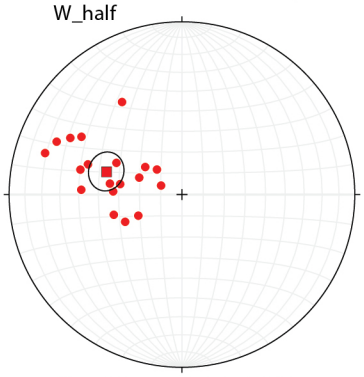

● n=20, m.v. = 017°, 38°SE
Cambrian-Ordovician

212. Bartley_Gleason_West_map_E_half

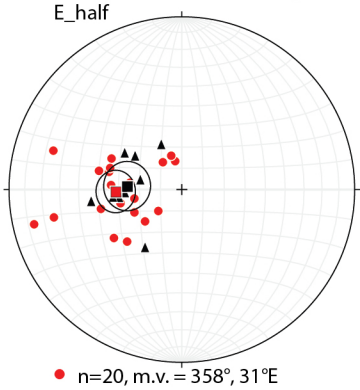

● n=20, m.v. = 358°, 31°E
Cambrian-Devonian
▲ n=9, m.v. = 004°, 26°E
Oligocene

213. Bartley_Gleason_West_map_E_half_rotated

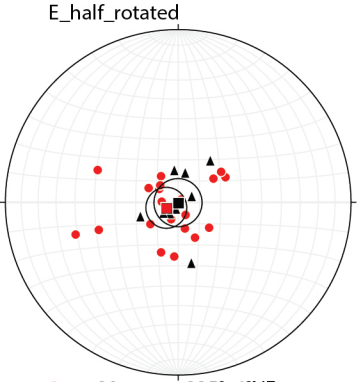

● n=20, m.v. = 335°, 6°NE
Cambrian-Devonian
Oligocene horizontal

214. Bartley_Gleason_East_map_N_third

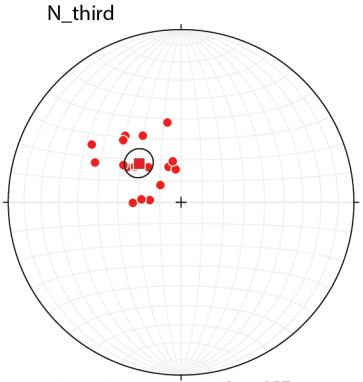

● n=18, m.v. = 043°, 27°SE
Ordovician-Devonian

215. Bartley_Gleason_East_map_middle_third

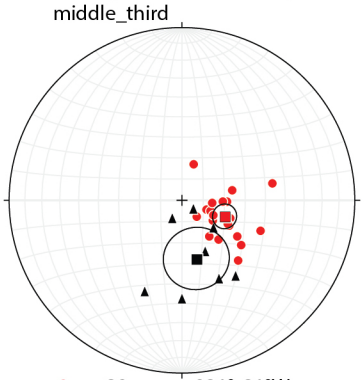

● n=20, m.v. = 021°, 21°W
Ordocivian-Devonian
▲ n=8, m.v. = 076°, 29°NW
Oligocene

216. Bartley_Gleason_East_map_middle_third_rotated

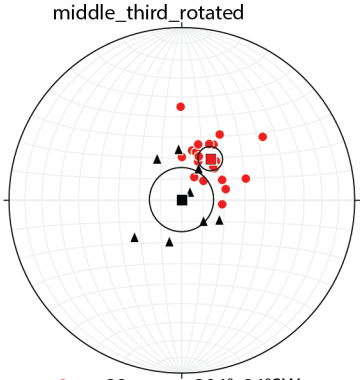

● n=20, m.v. = 304°, 24°SW
Ordocivian-Devonian
Oligocene horizontal

217. Bartley_Gleason_East_map_S_third

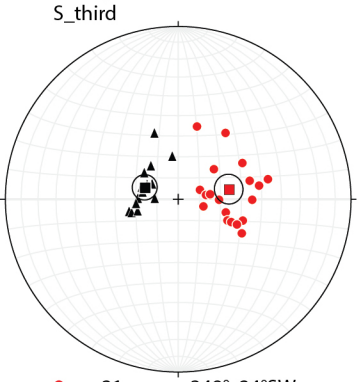

● n=21, m.v. = 349°, 24°SW
Ordocivian-Devonian
▲ n=14, m.v. = 020°, 17°SE
Oligocene

218. Bartley_Gleason_East_map_S_third_rotated

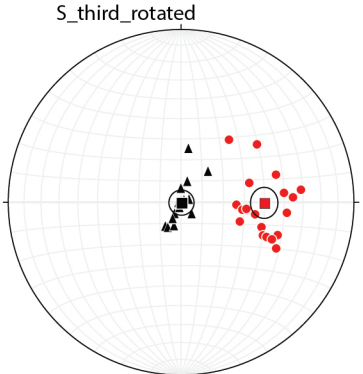

● n=21, m.v. = 000°, 40°W
Ordocivian-Devonian
Oligocene horizontal

219. Ekren_2012_SW_corner_N

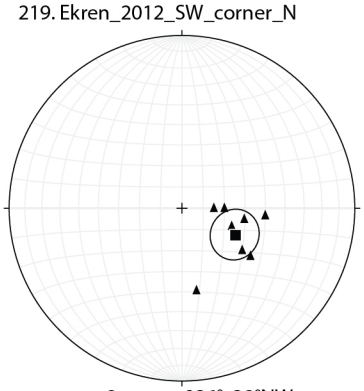

▲ n=8, m.v. = 026°, 28°NW
Oligocene

220. Ekren_2012_SW_corner_S

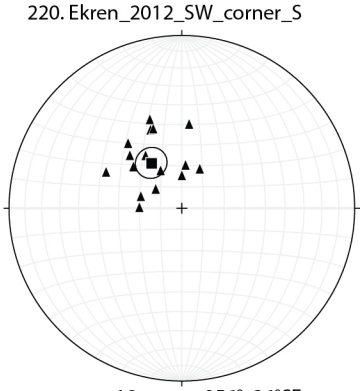

▲ n=18, m.v. = 056°, 26°SE
Oligocene

221. Ekren_2012_W_central

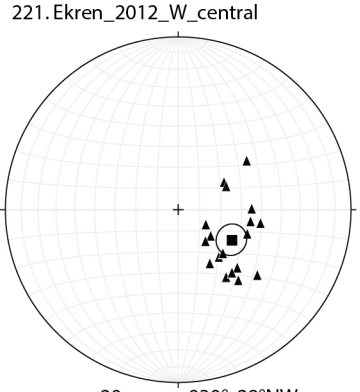

▲ n=20, m.v. = 030°, 29°NW
Oligocene

222. Ekren_2012_S_central

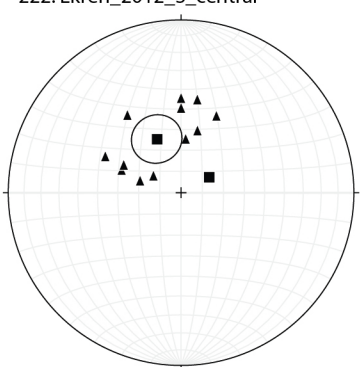

● n=1, m.v. = 330°, 15°SW
Ordocivian-Devonian
▲ n=13, m.v. = 066°, 28°SE
Oligocene

223. Ekren_2012_S_central_rotated

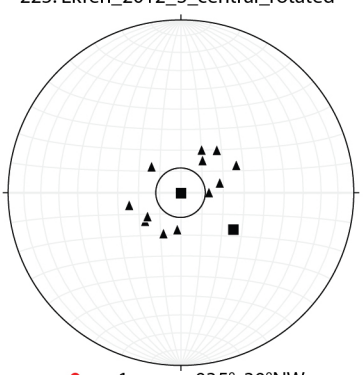

● n=1, m.v. = 035°, 30°NW
Ordocivian-Devonian
Oligocene horizontal

224. Feeley_N_half

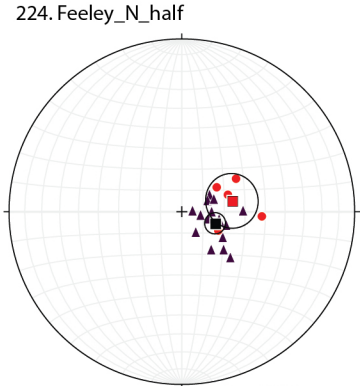

● n=5, m.v. = 348°, 24°SW
Permian
▲ n=16, m.v. = 019°, 17°NW
Oligocene

225. Feeley_N_half_rotated

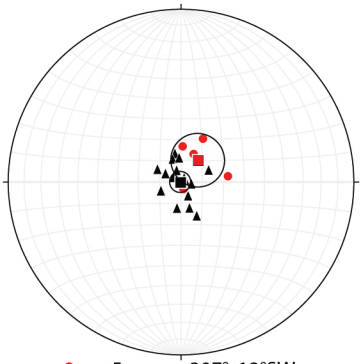

● n=5, m.v. = 307°, 13°SW
Permian
Oligocene horizontal

226. Feeley_S_half_W_third

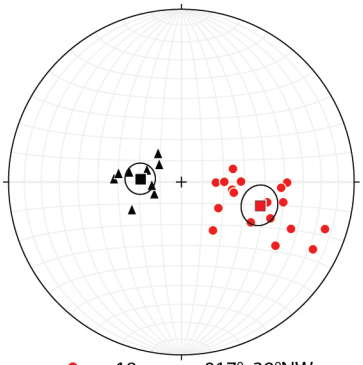

● n=18, m.v. = 017°, 39°NW
Permian
▲ n=9, m.v. = 005°, 19°E
Oligocene

227. Feeley_S_half_W_third_rotated

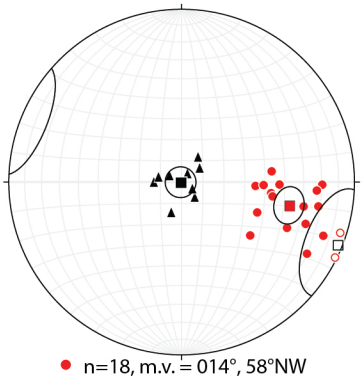

● n=18, m.v. = 014°, 58°NW
Permian
Oligocene horizontal

228. Feeley_S_half_middle_third

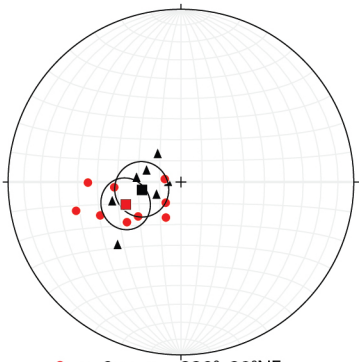

● n=9, m.v. = 339°, 28°NE
Permian
▲ n=7, m.v. = 350°, 19°E
Oligocene

229. Feeley_S_half_middle_third_rotated

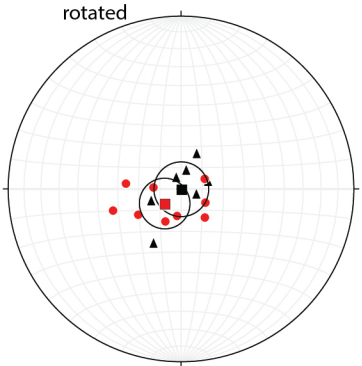

● n=9, m.v. = 318°, 10°NE
Permian
Oligocene horizontal

230. Feeley_S_half_E_third

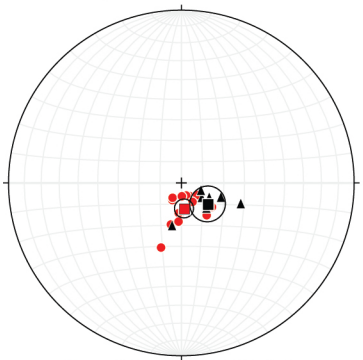

● n=15, m.v. = 084°, 12°N
Permian
▲ n=7, m.v. = 039°, 16°NW
Oligocene

231. Feeley_S_half_E_third_rotated

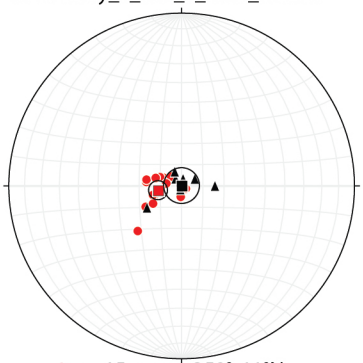

● n=15, m.v. = 350°, 11°N
Permian
Oligocene horizontal

232. Brokaw_Barosh_N_half_W_limb_Butte_syncline

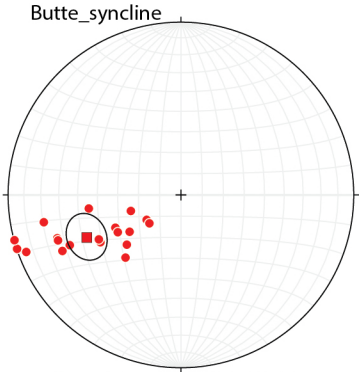

● n=19, m.v. = 336°, 50°NE
Permian

233. Brokaw_Barosh_N_half_E_limb_Butte_syncline

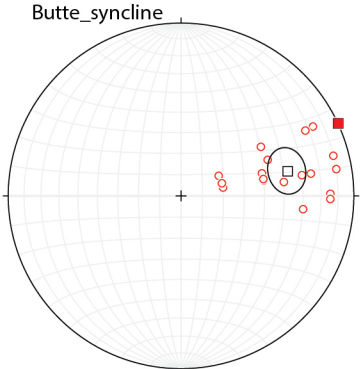

● n=20, m.v. = 345°, 57°SW
(overturned)
Pennsylvanian-Permian

234. Brokaw_Barosh_N_half_NE_corner

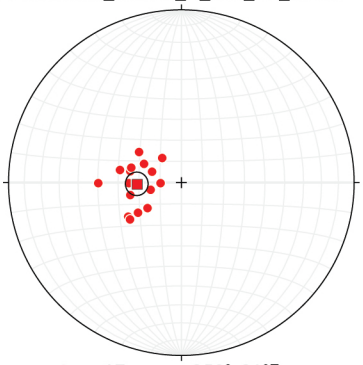

● n=17, m.v. = 359°, 21°E
Permian

235. Brokaw_Barosh_S_half_W_limb_Butte_syncline

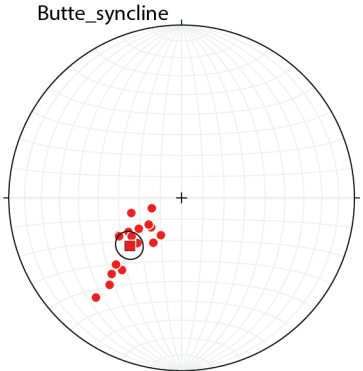

● n=18, m.v. = 318°, 34°NE
Permian

236. Brokaw_Barosh_S_half_E_limb_Butte_syncline

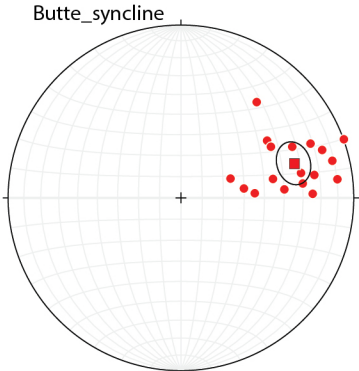

● n=18, m.v. = 343°, 58°SW
Pennsylvanian-Permian

237. Brokaw_Barosh_S_half_E_third

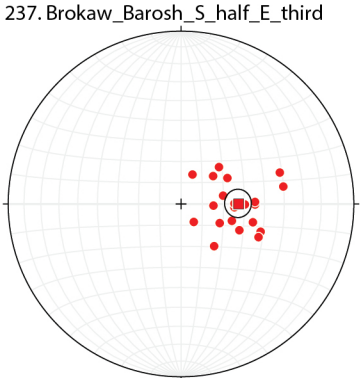

● n=22, m.v. = 359°, 27°W
Devonian-Pennsylvanian

238. Brokaw_Heidrich_NW_quarter

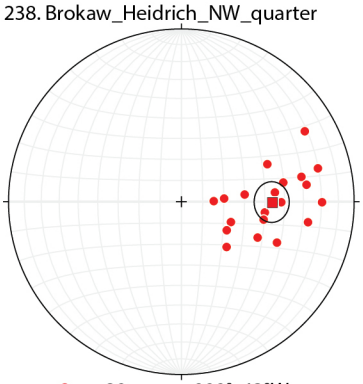

● n=20, m.v. = 000°, 43°W
Pennsylvanian-Permian

239. Brokaw_Heidrich_NE_corner_E_limb_Butte_syncline

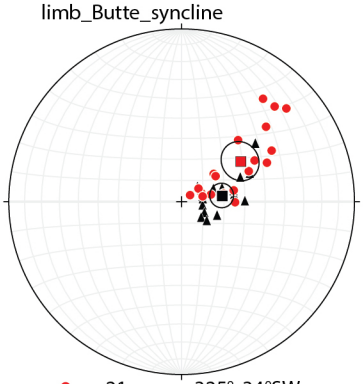

● n=21, m.v. = 325°, 34°SW
Permian
▲ n=17, m.v. = 351°, 19°W
Eocene-Oligocene

240. Brokaw_Heidrich_NE_corner_E_limb_Butte_syncline_rotated

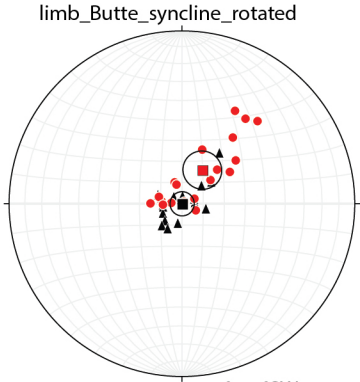

● n=21, m.v. = 301°, 19°SW
Permian
Eocene-Oligocene horizontal

241. Brokaw_Heidrich_SW_quarter

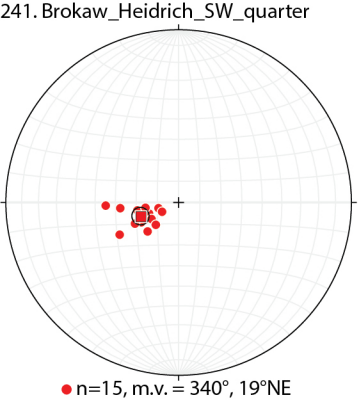

● n=15, m.v. = 340°, 19°NE
Pennsylvanian-Permian

242. Brokaw_S_central

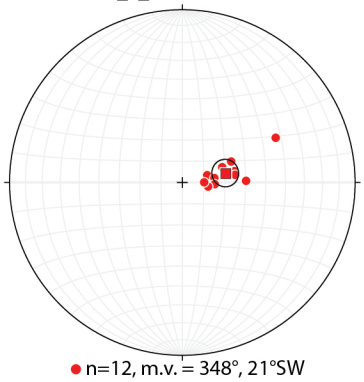

● n=12, m.v. = 348°, 21°SW
Permian

243. Overtoom_N_half

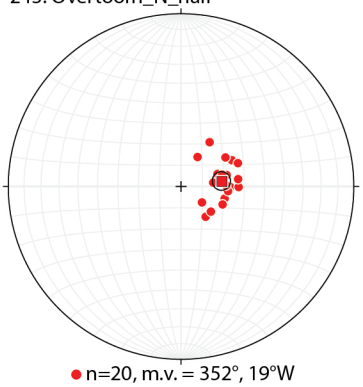

● n=20, m.v. = 352°, 19°W
Misssissippian-Permian

244. Overtoom_S_half

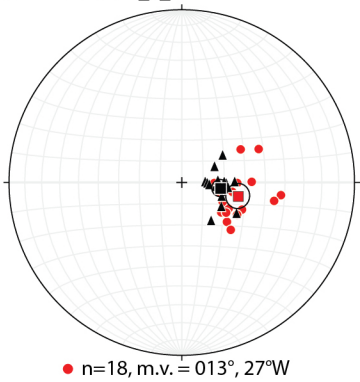

● n=18, m.v. = 013°, 27°W
Misssissippian-Permian
▲ n=16, m.v. = 008°, 18°W
Oligocene

245. Overtoom_S_half_rotated

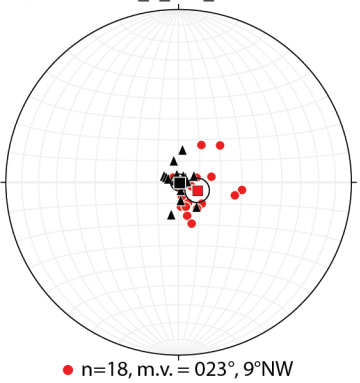

● n=18, m.v. = 023°, 9°NW
Misssissippian-Permian
Oligocene horizontal

246. Dubray_NE_corner

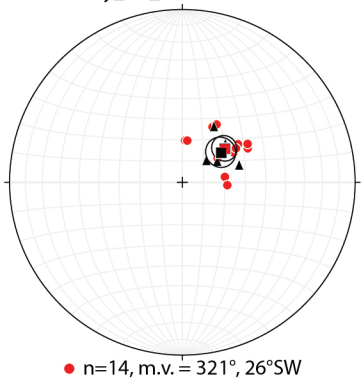

● n=14, m.v. = 321°, 26°SW
Devonian-Permian
▲ n=6, m.v. = 322°, 23°SW
Oligocene

247. Dubray_NE_corner_rotated

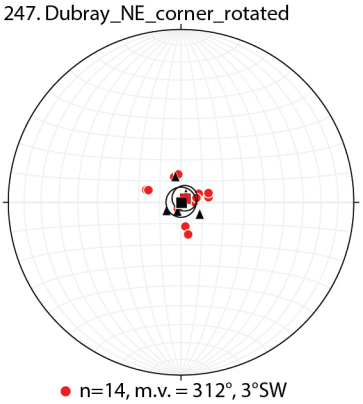

● n=14, m.v. = 312°, 3°SW
Devonian-Permian
Oligocene horizontal

248. Dubray_NW

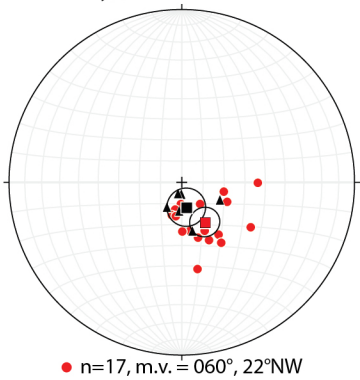

● n=17, m.v. = 060°, 22°NW
Devonian-Pennsylvanian
▲ n=6, m.v. = 080°, 12°N
Oligocene

249. Dubray_NW_rotated

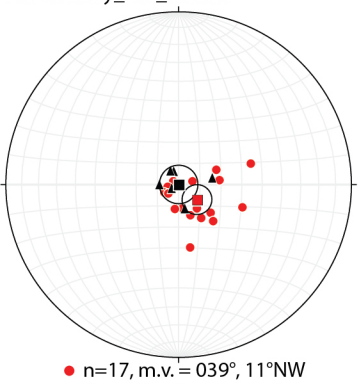

● n=17, m.v. = 039°, 11°NW
Devonian-Pennsylvanian
Oligocene horizontal

250. Dubray_center

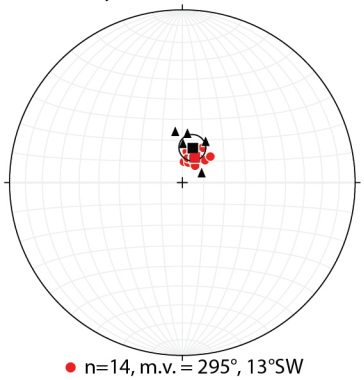

● n=14, m.v. = 295°, 13°SW
Devonian-Pennsylvanian
▲ n=7, m.v. = 296°, 17°SW
Oligocene

251. Dubray_center_rotated

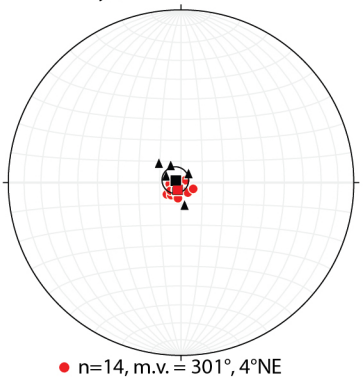

● n=14, m.v. = 301°, 4°NE
Devonian-Pennsylvanian
Oligocene rotated

252. Dubray_SW_quarter

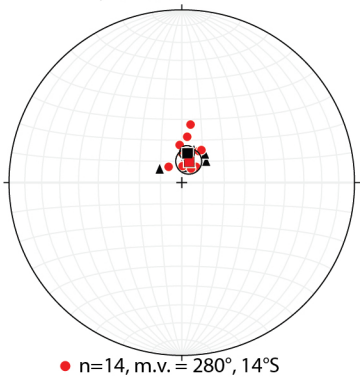

● n=14, m.v. = 280°, 14°S
Devonian-Mississippian
▲ n=7, m.v. = 288°, 11°SW
Oligocene

253. Dubray_SW_quarter_rotated

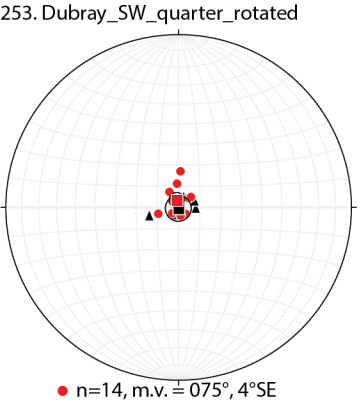

● n=14, m.v. = 075°, 4°SE
Devonian-Mississippian
Oligocene horizontal

254. Dubray_SE_quarter

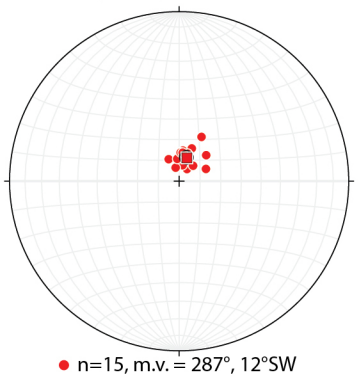

● n=15, m.v. = 287°, 12°SW
Devonian-Mississippian

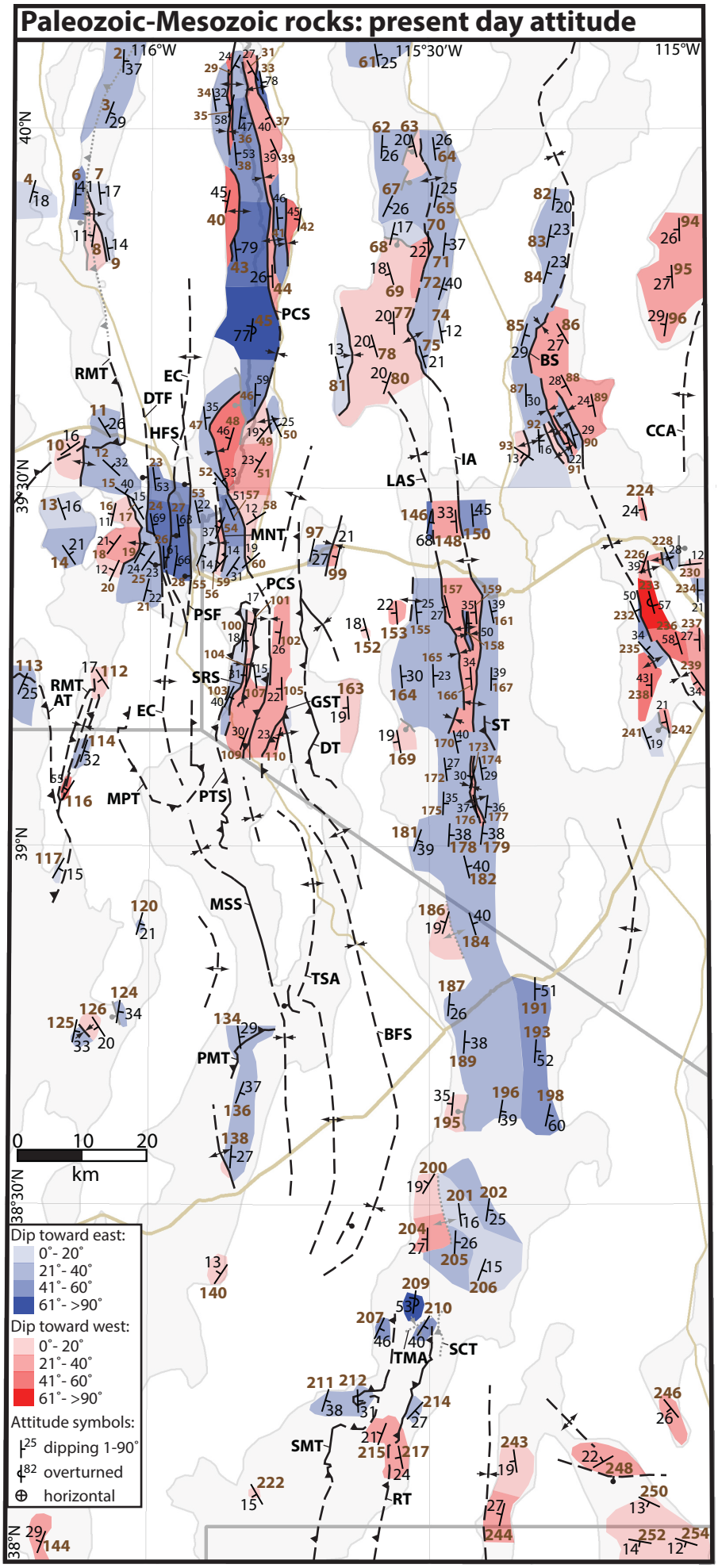
Paleozoic-Mesozoic rocks: present day attitude
116°W
115°30'W
115°W
40°N
39°30'N
39°N
38°30'N
38°N
RMT
EC
DTF
HFS
PCS
MNT
PSF
SRS
RMT AT
EC
MPT
PTS
GST
DT
MSS
TSA
BFS
PMT
IA
LAS
BS
CCA
ST
SCT
TMA
SMT
RT
0 10 20
km
Dip toward east:
0°- 20°
21°- 40°
41°- 60°
61°- >90°
Dip toward west:
0°- 20°
21°- 40°
41°- 60°
61°- >90°
Attitude symbols:
dipping 1-90°
overturned
horizontal

Plate 1

A. Correlation of map units

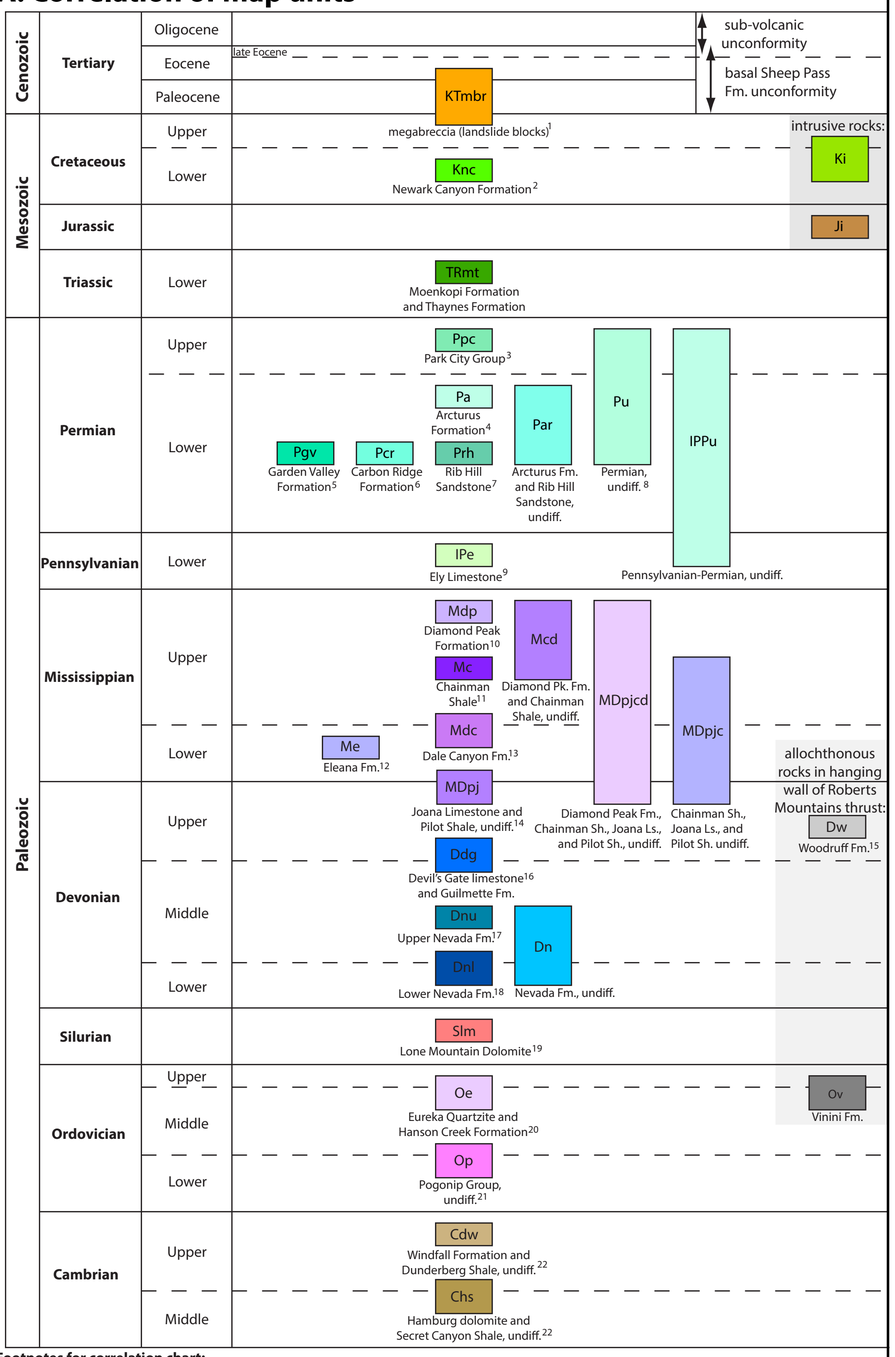

Footnotes for correlation chart:

1. Megabreccia units Klnc, Klcr, Kle, and Kln from Nolan et al. (1971) are mapped as KTmbr in the southern Diamond Mountains. In the Roberts Mountains, slide blocks of Ddg lying over Ov are mapped as KTmbr (McKee and Conrad, 1998).
2. Permian Unit G (Pgl, Pgu) from Larson and Riva (1963) mapped as Knc, after Stewart (1980), Stewart and Carlson (1978), and Haworth (1979).
3. Includes the Kaibab limestone, Gerster Formation (Douglass, 1960), and Plympton Formation (Connell, 1985), after Hose and Blake (1976).
4. Includes the Loray and Pequop formations (Connell, 1984), after Hose and Blake (1976).
5. Lies unconformably on either Mississippian rocks or Ordovician Vinini Formation (McKee and Conrad, 1998; Carlisle and Nelson, 1990)
6. Units Pa through Pf of Larson and Riva (1963) are mapped as Pcr after Hose and Blake (1976) and Roberts et al. (1967).
7. Includes Reipe Spring Limestone in Egan Range (Brokaw and Heidrick, 1966) and Pancake Range (Kleinhampl and Ziony, 1985).
8. Interpreted in drill holes in Railroad Valley, White River Valley, Long Valley, and White Pine Range (Hess et al., 2004).
9. Pennsylvanian Moleen Limestone and Tomera Formation of Campbell (1981) and Tomastik (1981) are mapped as IPe here.
10. Mdp is typically only divided out in source maps in the northwest quarter of the map area.
11. Includes unit Ms locally divided out by Kleinhampl and Ziony (1985), and unit Msw (Scotty Wash sandstone) of duBray and Hurtubise (1994).
12. Only in the southwest part of the map area. Ekren et al. (1973A) maps Me above Dn; Ddg was either not deposited here, or was eroded prior to Me deposition.
13. Units Mar and Marc of Hose (1983) are mapped as Mdc here, after stratigraphic divisions of Nolan et al. (1974). Mdc is local to Fish Creek and Diamond ranges. Also, in the Mahogany Hills, unit 'u' of Schalla (1978) (undifferentiated post-Devonian sandstone, shale, and conglomerate) is mapped here as Mdc, after Long et al. (2012).
14. Lower Mississippian Webb Formation (Mw) of Hose (1983) is mapped here as Joana Limestone.
15. Only mapped in Fish Creek Range; allochthonous Dw of Hose (1983) is interpreted as upper plate of Roberts Mountains allochthon, after Stewart and Carlson (1978).
16. Named Devil's Gate Limestone within and west of the Diamond Mountains, and Guilmette Formation to east and south; these two units are laterally-equivalent.
17. Includes Bay State Dolomite, Woodpecker Limestone, and Sentinel Mountain Dolomite members in the Diamond Mountains (Nolan et al., 1974), and Simonson Dolomite member elsewhere.
18. Includes Oxyoke Canyon Sandstone and Beacon Peak Dolomite members in Diamond Mountains (Nolan et al., 1974), and Oxyoke Canyon Sandstone member, Sadler Ranch Fm., McColley Canyon Fm., and Beacon Peak Dolomite member in Fish Creek Range (Hose, 1983; Cowell, 1986; Long et al., 2012). Consists of Sevy Dolomite in the majority of the map area, including Quinn Canyon Range and Railroad Valley (Ekren et al., 2012; Hess et al., 2004).
19. Includes the laterally-equivalent Laketown Dolomite mapped by Kleinhampl and Ziony (1985) and Ekren et al. (2012).
20. Includes Ely Springs Dolomite in Pancake and Quinn Canyon ranges (Kleinhampl and Ziony, 1985; Ekren et al., 2012); laterally-equivalent to Hanson Creek Dolomite.
21. Includes the Antelope Valley, Ninemile, and Goodwin Formations in the Fish Creek and Antelope Ranges (Hose, 1983; Long et al., 2012). Also includes the Copenhagen Formation of Hose (1983) in the southern Antelope Range.
22. Both Cdw and Chs are only exposed in the Fish Creek Range (Nolan et al., 1974; Long et al., 2012).

Abbreviations used in correlation chart:
undiff. = undifferentiated; Fm. = Formation; Sh. = shale; Ls. = limestone

B. Paleogene subcrop map of east-central Nevada

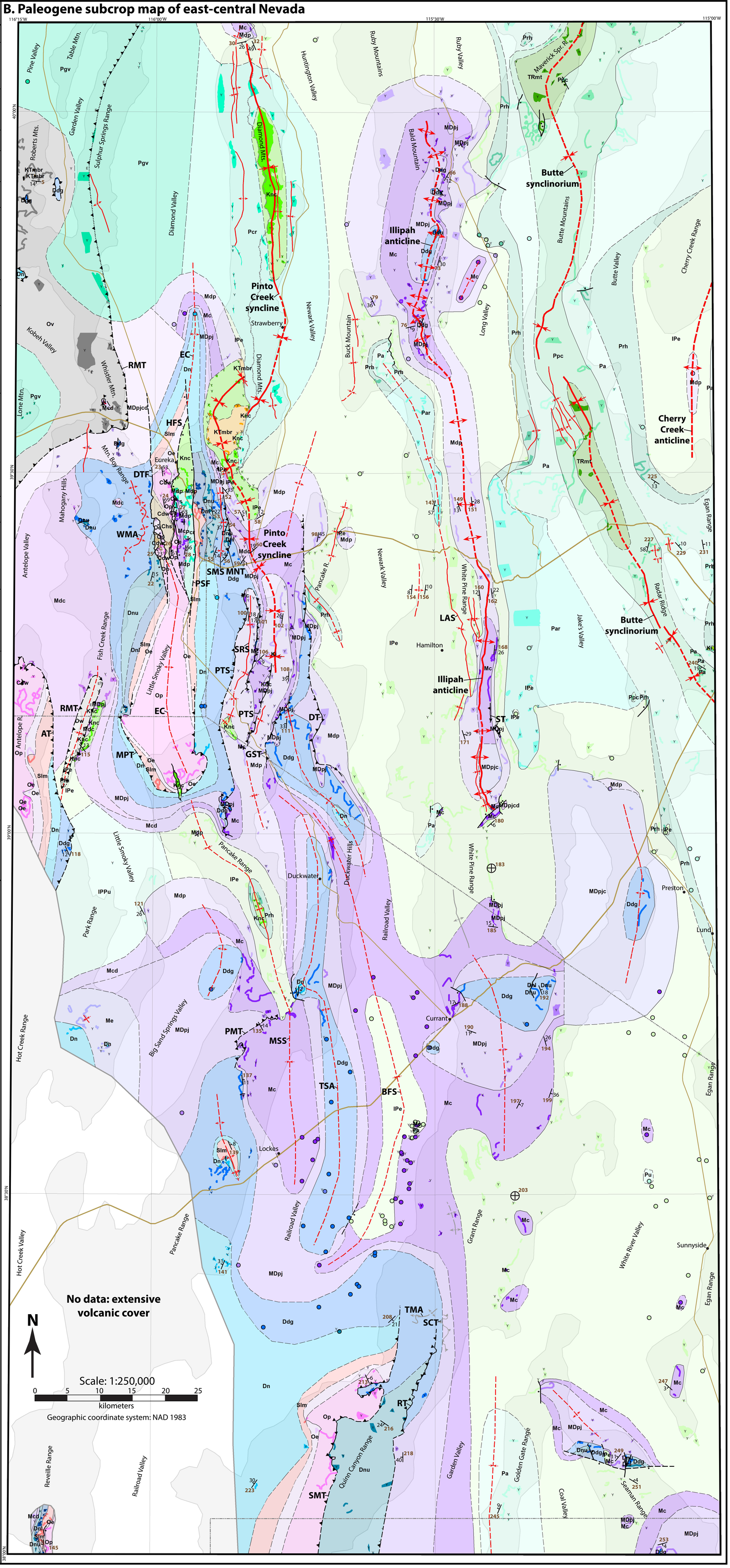

C. Geologic map sources

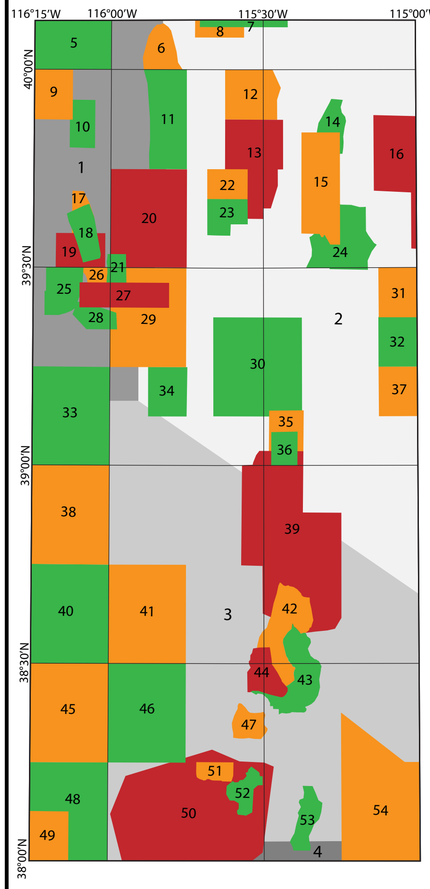

Source maps:

1 - Roberts et al. (1967)
2 - Hose and Blake (1976)
3 - Kleinhampl and Ziony (1985)
4 - Tschanz and Pampeyan (1970)
5 - Carlisle and Nelson (1990)
6 - Haworth (1979)
7 - Colgan et al. (2010)
8 - Millikan (1979)
9 - McKee and Conrad (1998)
10 - Lipka (1987)
11 - Larson and Riva (1963)
12 - Nutt and Hart (2004)
13 - Nutt (2000)
14 - Connell (1985)
15 - Otto (2008)
16 - Fritz (1968)
17 - Low (1982)
18 - Bentz (1983)
19 - Drake (1978)
20 - Nolan et al. (1971)
21 - Nolan (1962)
22 - Campbell (1981)
23 - Tomastik (1981)
24 - Douglass (1960)
25 - Schalla (1978)
26 - Simonds (1997)
27 - Long et al. (2012)
28 - Cowell (1986)
29 - Nolan et al. (1974)
30 - Humphrey (1960)
31 - Feeley (1993)
32 - Brokaw and Barosh (1968)
33 - Hose (1983)
34 - McDonald (1989)
35 - Guerrero (1983)
36 - Tracy (1969)
37 - Brokaw and Heidrick (1966)
38 - Dixon et al. (1972)
39 - Moores et al. (1968)
40 - Ekren et al. (1973A)
41 - Quinlivan et al. (1974)
42 - Lund et al. (1987)
43 - Lund et al. (1988)
44 - Camilleri (2013)
45 - Snyder et al. (1972)
46 - Ekren et al. (1972)
47 - Fryxell (1988)
48 - Ekren et al. (1973B)
49 - Martin and Naumann (1995)
50 - Ekren et al. (2012)
51 - Bartley and Gleason (1990)
52 - Bartley and Gleason (1990)
53 - Overtoom (1994)
54 - duBray and Hurtubise (1994)

D. Map explanation

Subcrop data:

- Subcrop beneath exposure of Paleogene unconformity
- Youngest possible subcrop beneath Paleogene unconformity
- Subcrop beneath Paleogene unconformity in drill hole
- Youngest possible subcrop beneath Paleogene unconformity in drill hole
- E — Easternmost exposure of rocks in hanging wall of Roberts Mountains thrust

Map symbols:

- anticline axis at Paleogene erosion surface
- syncline axis at Paleogene erosion surface
- axis of 1st-order Eastern Nevada fold belt anticline at Paleogene erosion surface
- axis of 1st-order Eastern Nevada fold belt syncline at Paleogene erosion surface
- anticline axis structurally below Paleogene erosion surface
- thrust fault (teeth on upthrown side)
- thrust fault structurally below Paleogene erosion surface (teeth on upthrown side)
- pre-unconformity normal fault (ball on downthrown side)
- post-unconformity normal fault (ball on downthrown side)
- stratigraphic contact between subcrop units
- road
- county boundary
- strike and dip of rocks during Paleogene; brown number corresponds to Figure SM1
- horizontal rocks during Paleogene; brown number corresponds to Figure SM1

Structure abbreviations:

Sulphur Springs Range and southern Fish Creek Range:
RMT - Roberts Mountains thrust
Antelope Range and Park Range:
AT - Antelope thrust
Fish Creek Range and Diamond Mountains:
EC - Eureka culmination
WMA - White Mountain anticline
DTF - Dugout Tunnel fault
HFS - Hoosac fault system
PSF - Pinto Summit fault
SMS - Sentinel Mountain syncline
MNT - Moritz-Nager thrust
Northern Pancake Range:
MPT - Moody Peak thrust
PTS - Pancake thrust system
SRS - Silverado Ridge syncline
GST - Green Springs thrust
DT - Duckwater thrust
Railroad Valley and southern Pancake Range:
PMT - Portuguese Mountain thrust
MSS - McClure Spring syncline
TSA - Trap Spring anticline
BFS - Bacon Flat syncline
White Pine Range and Bald Mountain:
ST - Shellback thrust
LAS - Little Antelope syncline
Grant Range and Quinn Canyon Range:
TMA - Timber Mountain anticline
SCT - Schofield Canyon thrust
RT - Rimrock thrust
SMT - Sawmill thrust